Biotechnology Advances 51 (2021) 107703

Contents lists available at ScienceDirect

Biotechnology Advances

journal homepage: www.elsevier.com/locate/biotechadv

Advances in enzymatic oxyfunctionalization of aliphatic compounds

Carmen Aranda [a,1,2], Juan Carro [b,1], Alejandro González-Benjumea [a], Esteban D. Babot [a], Andrés Olmedo [a], Dolores Linde [b], Angel T. Martínez [b,*], Ana Gutiérrez [a,*]

[a] Instituto de Recursos Naturales y Agrobiología de Sevilla (IRNAS), CSIC, Reina Mercedes 10, 41012 Seville, Spain
[b] Centro de Investigaciones Biológicas "Margarita Salas" (CIB), CSIC, Ramiro de Maeztu 9, 28040 Madrid, Spain

ARTICLE INFO

Keywords:
Peroxygenases
UPO
P450
Biocatalysis
Oxyfunctionalization
Hydroxylation
Epoxidation
Alkanes
Fatty acids
Terpenoids

ABSTRACT

Selective oxyfunctionalizations of aliphatic compounds are difficult chemical reactions, where enzymes can play an important role due to their stereo- and regio-selectivity and operation under mild reaction conditions. P450 monooxygenases are well-known biocatalysts that mediate oxyfunctionalization reactions in different living organisms (from bacteria to humans). Unspecific peroxygenases (UPOs), discovered in fungi, have arisen as "dream biocatalysts" of great biotechnological interest because they catalyze the oxyfunctionalization of aliphatic and aromatic compounds, avoiding the necessity of expensive cofactors and regeneration systems, and only depending on H_2O_2 for their catalysis. Here, we summarize recent advances in aliphatic oxyfunctionalization reactions by UPOs, as well as the molecular determinants of the enzyme structures responsible for their activities, emphasizing the differences found between well-known P450s and the novel fungal peroxygenases.

1. Introduction

The activation of C—H bonds in aliphatic and other compounds for their oxyfunctionalization is of great interest for the chemical industry. Those bonds are thermodynamically strong and rather inert and, therefore, their activation is an intricate task (Balcells et al., 2010; Wang et al., 2017; Xue et al., 2017). Not only is the activation of the said bonds difficult, but also that of molecular oxygen is hindered due to its ground triplet state. Transition metals are currently employed for this purpose, but the outcome of the reactions is not desirable due to the poor selectivity they display (Roduner et al., 2013), so biocatalysis can present different advantages.

The addition of oxygen to aliphatic hydrocarbons and biobased lipids, which are cheap and widespread feedstocks, may convert them into very valuable compounds, such as building blocks or pharmaceuticals. In this review, we will focus in two types of oxygenation reactions, namely hydroxylation and epoxidation. The reaction of hydroxylation is one of the most common ways of drug metabolism leading to: **i)** detoxification processes by increasing hydrophilicity of more hydrophobic compounds for subsequent excretion; or **ii)** bioactivation processes producing reactive metabolites. The "*in vitro*" synthesis of these compounds is of interest for the production of new more active drugs and for the safety testing of their metabolites in the organism to assess human risks and ensure clinical safety of new therapeutic agents (Atrakchi, 2009; Baillie et al., 2002). On the other hand, epoxidation and other oxygenation reactions are under the spotlight due to the current and potential commercial applications of the obtained products. Epoxides from vegetable oils and their hydrolysis or transesterification products are of interest for several industrial applications such as stabilizers and plasticizers (Jia et al., 2016; Kandula et al., 2014), and are also promising intermediates for the production of polyols (Zhang et al., 2014a), polyurethanes (Zhang et al., 2014b), biolubricants (Borugadda and Goud, 2014) and epoxy resins (Xia and Larock, 2010), among other uses.

The main advantage of using biocatalysis in the synthesis of these compounds is the enzymatic selectivity, which is in contrast with the use of small-molecule chemical catalysts. Normally, enzymes engulf the substrates in such a way that their positioning inside the catalyst restricts the regions that can be altered. Thus, regio- and even stereoselectivity arises. Moreover, the economic and environmental benefits that make biocatalytic methods attractive include the biodegradable and nontoxic nature of biocatalysts and their ability to perform their

* Corresponding authors.
E-mail addresses: atmartinez@cib.csic.es (A.T. Martínez), anagu@irnase.csic.es (A. Gutiérrez).
[1] These two authors equally contributed to the work.
[2] Current address: Johnson Matthey, Cambridge Science Park U260, Milton Road, Cambridge CB4 0FP, UK.

https://doi.org/10.1016/j.biotechadv.2021.107703
Received 7 November 2020; Received in revised form 17 January 2021; Accepted 25 January 2021
Available online 3 February 2021

selective reactions under mild conditions (Sheldon and Woodley, 2018). Thanks to advances in genetic and protein engineering, allowing for the easier production of better biocatalysts, and the new methods of reaction engineering (Wohlgemuth, 2017; Woodley, 2019), biocatalytic methods are emerging as an alternative to traditional synthetic chemistry. As a consequence, the amount of processes able to be carried out at preparative scales (even in some cases at industrial scale) is continuously growing (Chakrabarty et al., 2020; Wiltschi et al., 2020). However, the use of biocatalysts also presents some disadvantages. In general, enzymes introducing oxygen atoms display rather low turnover numbers due to their intrinsic complex mechanisms, often require multiprotein interactions and cofactors and, in many cases, there exist uncoupling of electron transfer and product formation, giving rise to reactive oxygen species (Girhard et al., 2015; Holtmann and Hollmann, 2016).

In this review, we highlight the advances in enzymatic oxyfunctionalization of a number of aliphatic compounds and the current availability of new and promising oxygenation biocatalysts. Special emphasis is made on the reactions catalyzed by the self-sufficient unspecific peroxygenases (UPOs), which have been termed "dream biocatalysts" owing to their unique features (Wang et al., 2017) that make them an appealing starting point for biotechnological applications. Moreover, comparison with other oxygenases, such as cytochrome P450 monooxygenases (P450s), is included in some cases. In addition to the reactions that these enzymes catalyze, a smattering of their structure-function relationships, as well as the biotechnological efforts to render them better biocatalysts, are provided.

2. Oxyfunctionalization biocatalysts

Oxygenases are biocatalysts able to transfer one oxygen atom (in the case of monooxygenases, where the second oxygen is reduced to water) or two oxygen atoms (thus known as dioxygenases, not included in the present review) from O_2 (*e.g.* the well-known P450s) or H_2O_2 (*e.g.* the more recently discovered UPOs, also acting as monooxygenases) to different substrates (Fig. 1) introducing new functionalities into them. These enzymes are of great interest for synthetic chemistry since they can act even on the most chemically inert positions of aliphatic and other compounds (Dong et al., 2018).

2.1. Classical monooxygenases

Monooxygenases are the main natural biocatalysts to mediate oxyfunctionalizations, being P450s the largest and most diverse group (Munro et al., 2018). P450s are heme-containing enzymes that catalyze the insertion of one atom of oxygen (Fig. 2) through the electrophilic species Compound I. Most P450s require nicotinamide cosubstrates and NAD(*P*)H-driven redox partners for function, to transform the hydride donation from NAD(*P*)H into two consecutively single electron transfer enabling O_2 activation and formation of compound I.

There are some P450s, grouped into classes VII and VIII, that possess both the P450 (heme) and the reductase domains fused, which makes them of high relevance for synthetic chemistry (Ciaramella et al., 2017). Typical examples of these enzymes are the $P450_{RhF}$ from *Rhodococcus* sp. (Roberts et al., 2003) and the naturally-fused and more studied P450 from *Bacillus megaterium* ($P450_{BM3}$), the first of this kind to be described (Whitehouse et al., 2012). Other naturally fused ("self-sufficient") enzymes mentioned in this review are the P450s from *Labrenzia aggregata* ($P450_{LaMO}$) (Yin et al., 2014) and those found in thermophilic *Amycolatopsis thermoflava*, *Jahorihella thermophila* and *Thermobispora bispora* (Tavanti et al., 2018). Besides, artificial chimeric proteins have been constructed in which the P450 catalyst of interest and a reductase domain of choice are fused. This simplifies the catalysis to the only

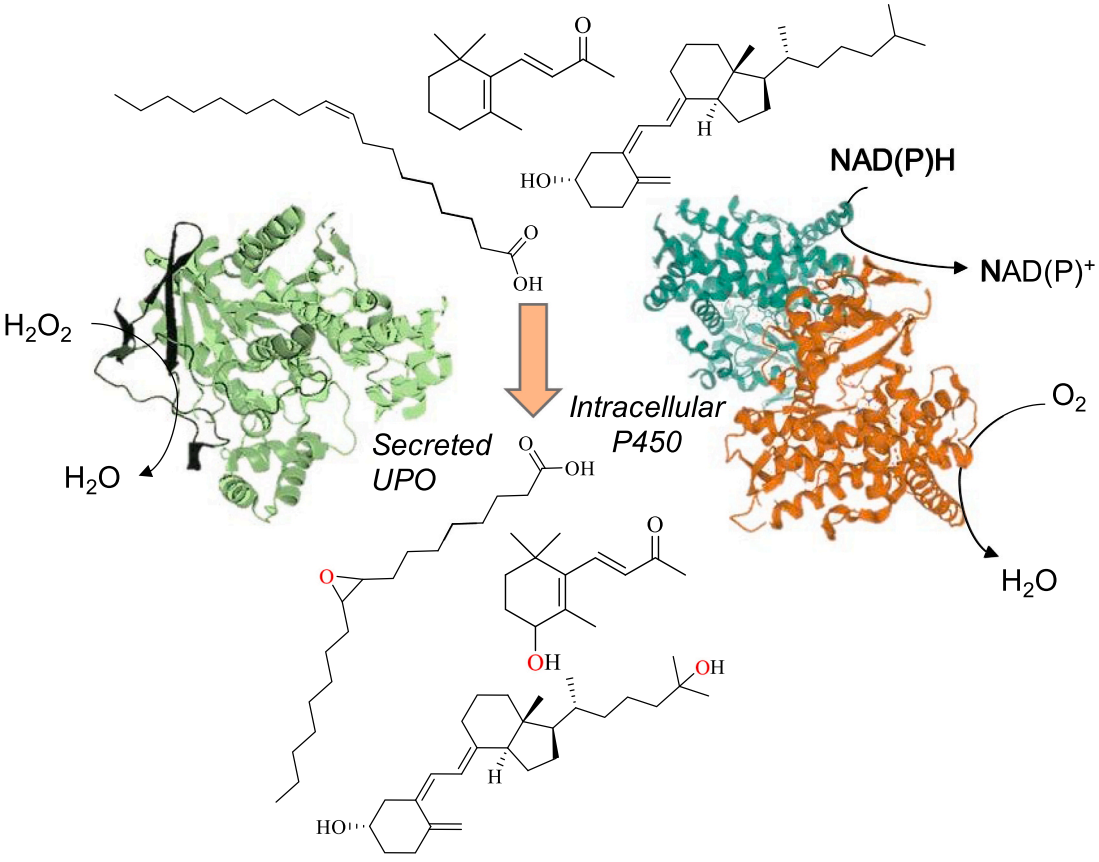

Fig. 1. Aliphatic oxyfunctionalizations by classical two-domain P450s and fungal UPOs differing in their intra- or extra-cellular location, the former being associated with lower operational stability and dependence on a source of reducing power.

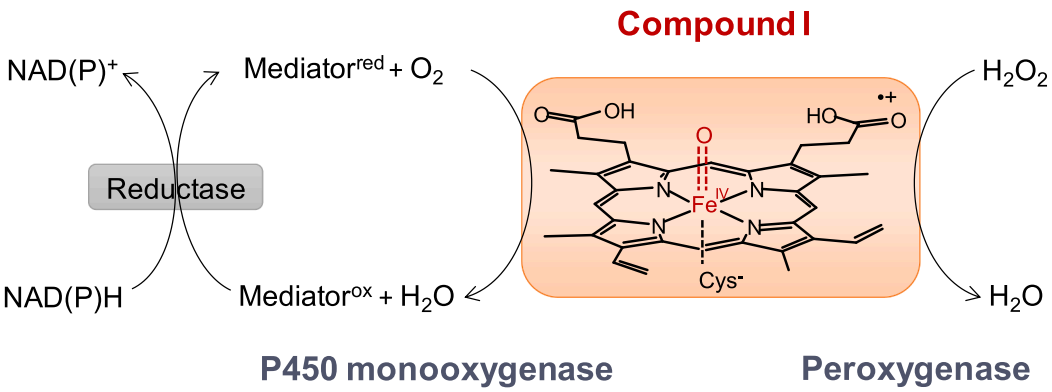

Fig. 2. Comparison of reactive compound I formation by reductive activation of O_2 in classical P450s or by H_2O_2 in peroxygenases.

addition of NAD(*P*)H for a specific function (Kubota et al., 2005; Pennec et al., 2015; Robin et al., 2011; Sadeghi and Gilardi, 2013).

Beyond these natural or artificial fusion enzymes, there are some P450s, the so-called "P450 peroxygenases", able to form the compound I directly from H_2O_2 through the so-called 'peroxide shunt' in a two-electron transfer avoiding the necessity of the redox partners (Girvan et al., 2007). The first P450-peroxygenases discovered were $P450_{SP\alpha}$ from *Sphingomonas paucimobilis* (Matsunaga et al., 1994), $P450_{BS\beta}$ from *Bacillus subtilis* (Matsunaga et al., 1999) and $P450_{CLA}$ from *Clostridium acetobutylicum* (Girhard et al., 2007). Artificial H_2O_2-dependent P450 systems have also been constructed by protein engineering or using decoy molecules to facilitate the catalysis (Fujishiro et al., 2012; Li et al., 2001) although they usually exhibit lower activity than those of the reductive oxygen activation process. While with $P450_{BM3}$ efficient systems have been reported that even work at kilogram scale (Kaluzna et al., 2016), processes with P450-peroxygenases proceed with low efficiency and lead to easier enzyme inactivation (Munro et al., 2018).

Apart from heme-dependent oxygenases, including plant peroxygenases (Hamberg and Fahlstadius, 1992) together with P450s, there are flavin-dependent monooxygenases oxyfunctionalizing aliphatic compounds through a flavin C4a-oxygen adduct (Huijbers et al., 2014). Baeyer-Villiger monooxygenases (BVMOs) and styrene monooxygenases (SMOs) are notable examples of this. Some BVMOs are dependent on reducing power for the regeneration of their flavin cofactor, whereas others do so by oxidizing other substrates (Bucko et al., 2016). On the other hand, SMOs rely on a two-component system, a flavin reductase and the monooxygenase itself, which are sometimes separate enzymes or different domains of the same enzyme (Fabara and Fraaije, 2020). BVMOs catalyze the oxidation of carbonylic substrates to ester or lactone products NADPH-dependently, although their ability to catalyze other oxidations such as sulfoxidations and epoxidations has also been reported (de Gonzalo et al., 2010). On the other hand, SMOs classically convert styrene derivatives to the corresponding (*S*)-styrene oxides. However, the substrate scope could be enlarged by protein engineering and the emergence of new SMOs (Lin et al., 2012; Toda et al. 2012a, 2012b and 2015).

2.2. New unspecific peroxygenases (UPOs)

Since their discovery in 2004 in the basidiomycete *Agrocybe aegerita* (Ullrich et al., 2004), heme-containing fungal UPOs have gained enormous attention as oxyfunctionalization biocatalysts due to their biotechnological potential since they are functionally similar to P450s, with compound I as oxygenating species, but they do not need expensive cofactors nor redox partners for function (Fig. 2). In addition, these enzymes are extracellular proteins, which confers them higher stability compared to intracellular or membrane-bound enzymes (such as many P450s or plant seed peroxygenases) and they are also easily recovered in high yields from the fungal cultures (Gröbe et al., 2011).

Some of the main advances produced and different milestones attained in UPO studies are summarized in Fig. 3. Fungal peroxygenases were first described as haloperoxidases (*A. aegerita* peroxidases, AaP) or aromatic peroxygenases (APO) because of the hydroxylation activity found on halides and aromatic compounds, respectively (Ullrich et al., 2004; Ullrich and Hofrichter, 2005). However, they were finally established as unspecific peroxygenases (UPOs, EC 1.11.2.1) after their activity was also demonstrated on aliphatic compounds (Gutiérrez et al., 2011; Peter et al., 2011). In the past years, several wild type UPOs have been described in basidiomycetes such as *Agrocybe aegerita* (*Aae*UPO), *Coprinellus radians* (*Cra*UPO), *Marasmius rotula* (*Mro*UPO), *Marasmius wettsteinii* (*Mwe*UPO) (Anh et al., 2007; Gröbe et al., 2011; Ullrich et al., 2004 and 2018) and ascomycetes such as *Chaetomium globosum* (*Cgl*UPO) (Kiebist et al., 2017). Their widespread occurrence in the fungal kingdom was demonstrated during the study of fungal genomes in which several-thousand peroxygenase-type genes were identified (Hofrichter et al., 2015) allowing for the production of recombinant enzymes like those from *Coprinopsis cinerea* (r*Cci*UPO) (Babot et al., 2013) and *Humicola insolens* (r*Hin*UPO) (Kiebist et al., 2017), heterologously expressed by Novozymes A/S in *Aspergillus oryzae,* and the ones from *Marasmius rotula* (r*Mro*UPO), *Collariela virescens* (r*Cvi*UPO) and *Daldinia caldariorum* (r*Dca*UPO) expressed in *Escherichia coli* (Carro et al., 2019; Linde et al., 2020). One of the most exciting features of UPOs is their catalytic versatility with more than 300 substrates already reported including reactions of oxyfunctionalizations (Aranda et al., 2018b; Babot et al., 2015a; Carro et al., 2015, 2018; Karich et al., 2013; Kinne et al., 2008 and 2010; Kluge et al., 2012; Peter et al., 2013; Ullrich et al., 2008), ether cleavage (Kinne et al., 2009), fatty-acid chain shortening (Olmedo et al., 2017) and side-chain removal of corticosteroids (Ullrich et al., 2018), among others described below.

Another fungal heme-thiolate protein closely related to UPOs is the chloroperoxidase (CPO) from the ascomycete *Leptoxyphium fumago* (syn. *Caldaromyces fumago*). This enzyme typically performs halide oxidation and its peroxygenase activity is limited to epoxidation of styrene (Tuynman et al., 2000) and linear alkenes (Geigert et al., 1986), moderate hydroxylation of benzylic carbons (Miller et al., 1995) and sulfoxidations (Colonna et al., 1992; Manoj and Hager, 2001), while it is unable to perform oxygenation of stronger C—H bonds.

3. Aliphatic oxyfunctionalization by UPOs

Aliphatic oxyfunctionalization reactions with UPOs have been described on a wide variety of substrates and, in most cases, with different regioselectivity depending on the enzyme used. Some of the most relevant reactions, with representative examples, are detailed in the following subsections and compared with similar reactions catalyzed by some P450s.

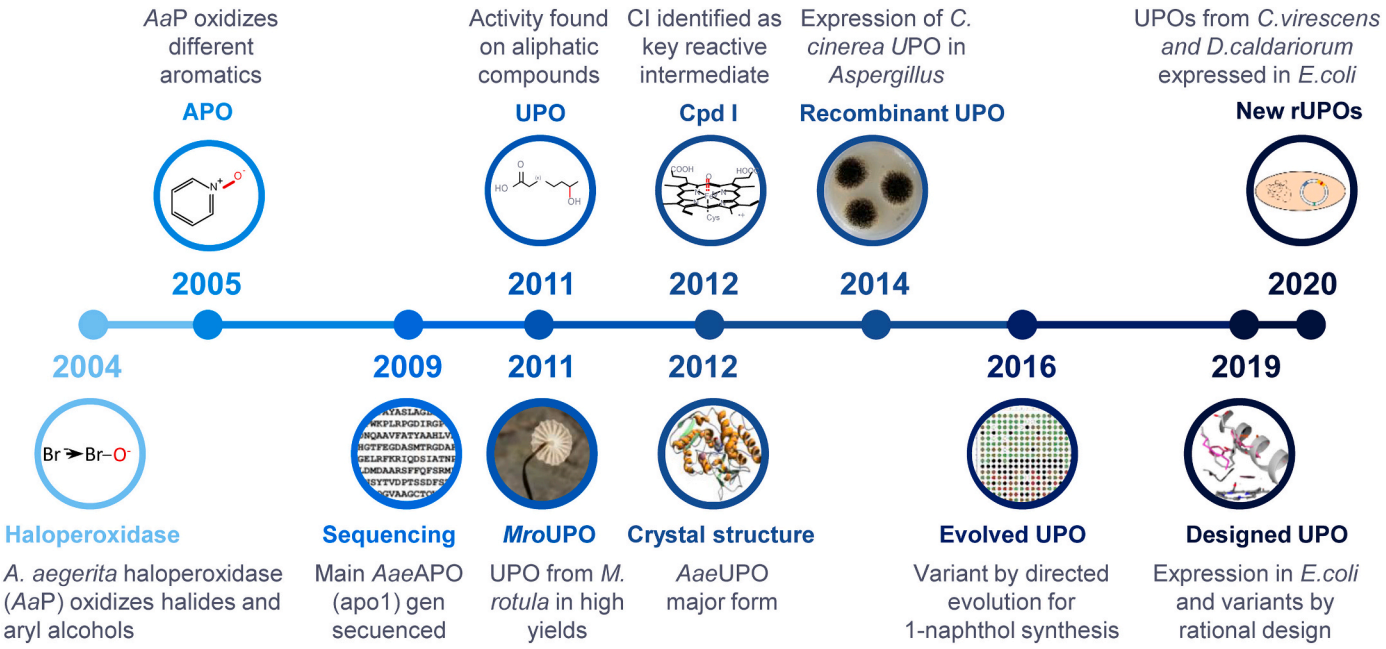

Fig. 3. Timeline of most relevant events and milestones in the history of fungal UPOs.

Table 1
Benzylic oxygenations by UPOs and some P450s.

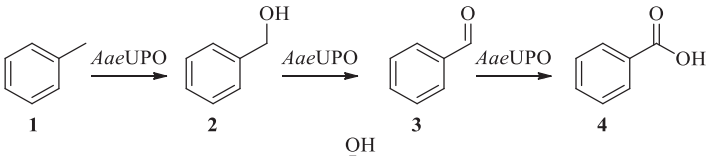	(Kinne et al., 2010; Ullrich and Hofrichter, 2005)
	(Kluge et al., 2012)
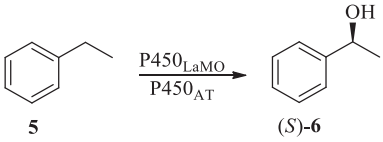	(Tavanti et al., 2018; Yin et al., 2014)
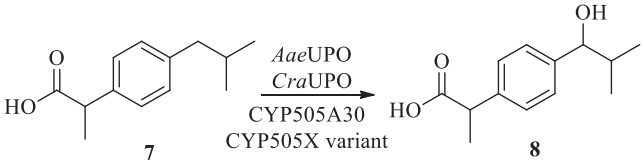	(Poraj-Kobielska et al., 2011) (Fürst et al., 2019; Rinnofner et al., 2019)
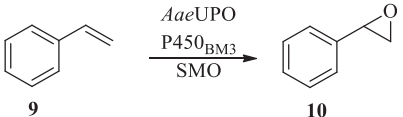	(Kluge et al., 2012) (Rauch et al., 2019)
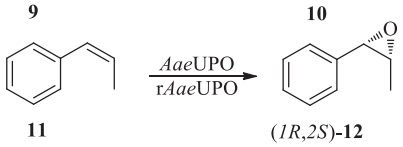	
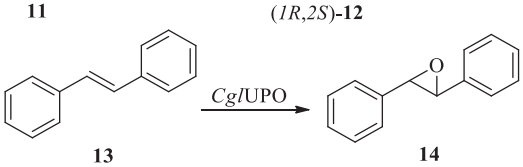	(Aranda et al., 2018d)

3.1. Benzylic oxygenation

Relevant examples of benzylic oxygenations by UPOs and some P450s are outlined in Table 1. The first aliphatic oxygenations reported for UPOs were targeted on the benzylic position of alkyl-benzenes. The resulting reaction was first described for toluene (**1**), in which hydroxylation in the phenyl moiety was also observed, yielding the alcohol (**2**), aldehyde (**3**) and acid (**4**) products from the predominant benzylic oxidation (Kinne et al., 2010; Ullrich and Hofrichter, 2005). Interestingly, when the methyl group of toluene is exchanged for a larger group like ethyl, propyl or butyl, the hydroxylation takes place exclusively in the alkyl chain (Kluge et al., 2012). The stereoselective hydroxylation of ethylbenzene (**5**) to (*R*)-1-phenylethanol ((*R*)-**6**) by *Aae*UPO was first reported in 2012 (Kluge et al., 2012), attaining a total turnover number (TTN) of 43,000, and it has been used as the model reaction for engineering UPO reactions ever since. As another example, Hollmann's group established two-liquid phase systems and non-aqueous reaction conditions using the recombinant enzyme (PaDa-I mutated variant of *Aae*UPO) produced in *Komagataella pastoris* (syn. *Pichia pastoris*) for this reaction (Fernández-Fueyo et al., 2016). The former two-liquid phase conditions permitted the enzyme to attain 200,000 TTN. The latter was demonstrated on semi-preparative scale (250 ml), yielding 1.25 g of enantiopure (*R*)-1-phenylethanol, where the immobilized biocatalyst was able to attain 90,000 TTN thanks to the above setup. Interestingly, the stereoselectivity of the reaction was towards the (*R*)-enantiomer ((*R*)-**6**, >99% enantiomeric excess, *ee*), while using $P450_{LaMO}$, the opposite enantiomer ((*S*)-**6**, 99% *ee*) was produced (Yin et al., 2014). Other self-sufficient P450s from *A. thermoflava*, *J. thermophila* and *T. bispora* also catalyzed this reaction with (*S*)-stereoselectivity but with lower *ee* values (Tavanti et al., 2018). Small overoxidation in the hydroxylation of ethylbenzene was observed with both *Aae*UPO (<5%) and $P450_{LaMO}$ (18%).

One interesting application of benzylic hydroxylation is the production of the ibuprofen (**7**) active metabolite 2-hydroxyibuprofen (**8**). This reaction has been performed by *Cra*UPO and *Aae*UPO with higher yield (74%) and regioselectivity (75%) for the former enzyme (Poraj-Kobielska et al., 2011). The same reaction was performed on semi-preparative scale (150–500 mg of starting material) by analogues of $P450_{BM3}$ such as CYP505A30 (Fürst et al., 2019) and a mutated variant of CYP505X (Rinnofner et al., 2019). In the first case, 15% (22 mg) of the desired product was obtained after 9 h of reaction, while in the second, 37% (180 mg) yield was attained after 22 h.

Another interesting example for synthetic chemistry is the epoxidation of styrenes for building blocks (McKenna et al., 2013). Styrene (**9**) epoxidation by wild-type (WT) $P450_{BM3}$ and *Aae*UPO exhibited low or null stereoselectivity (Huang et al., 2011; Kluge et al., 2012). However, it was improved by structure-based mutagenesis of $P450_{BM3}$ to attain a 64% *ee* towards the (*R*)-enantiomer of styrene oxide (**10**). The opposite (*S*)-enantiomer could be synthesized by the P450-peroxygenase $P450_{SP\alpha}$ in the presence of (*R*)-ibuprofen as "decoy molecule", achieving *ee* from moderate (63% for the WT) to high (88% for the F288G variant) (Fujishiro et al., 2012). However, the highest stereoselectivity in styrene epoxidation is achieved by the FAD-containing SMOs (Liu et al., 2016b; Mooney et al., 2006). Although the epoxidation of styrene by *Aae*UPO proceeded with low stereoselectivity, the opposite was observed with *cis*-β-methylstyrene (**11**) catalyzed with >99% *ee* towards (*1R,2S*)-epoxystyrene (**12**) (Kluge et al., 2012). This reaction was later performed by the recombinant r*Aae*UPO in neat substrate to increase the productivity and space-time yields (Rauch et al., 2019) and was applied to building an interesting chemoenzymatic cascade to afford the valuable drug (pseudo)ephedrine. Besides, the applicability of the neat system was demonstrated during the epoxidation of several other styrene derivatives (Rauch et al., 2019).

Among different UPOs, epoxidation of the bulkier molecule of stilbene (**13**) was only reported for *Cgl*UPO (Aranda et al., 2018d) forming the side-chain epoxide (**14**) while other UPOs —such as *Aae*UPO, r*Cci*UPO and *Mro*UPO— hydroxylated the aromatic moieties instead of oxygenating the aliphatic chain. SMO failed to oxygenate this substrate (Liu et al., 2016b).

3.2. Fatty acid and fatty alcohol oxygenation

Relevant examples of oxygenations of fatty acids and fatty alcohols by UPOs and some P450s are summarized in Table 2. Hydroxyfatty acids are another example in which the oxygenated derivatives are valuable compounds for the chemical, food, cosmetic and biofuel industries. Fatty acids are gaining importance as building blocks since they can be easily obtained from biomass (vegetable oils) in such a purity to be used for subsequent chemical or enzymatic transformations. The insertion of a hydroxyl group confers new properties to these compounds such as more reactivity and more solvent miscibility. Hydroxyfatty acids are used in the synthesis of polymers, resins and soaps, as additives in lubricant oils and paints, and as raw material for glue and surface coating production (Metzger and Bornscheuer, 2006; Mutlu and Meier, 2010; Tiran et al., 2008). Saturated fatty acid (C12-C18, **15**) hydroxylation was catalyzed by *Aae*UPO and r*Cci*UPO in ω-1 (**16**) and ω-2 (**17**) positions to form a mixture of monohydroxylated derivatives (Babot et al., 2013; Gutiérrez et al., 2011) while *Mro*UPO showed activity even on the most inert terminal position as observed during the oxidation of dodecanoic and tetradecanoic acids, forming the dicarboxylic acid (**19**), together with the ω-1-keto (**18**) derivative, as main reaction products (Olmedo et al., 2016). P450s have been reported to hydroxylate saturated fatty acids similarly to UPOs as recently reviewed by Hammerer et al. (2018). For example, the most studied $P450_{BM3}$ enables the hydroxylation of C12-C20 fatty acids at the ω-1, ω-2 and ω-3 positions similarly to UPOs (Miura and Fulco, 1975). Meanwhile, hydroxylation of fatty acids in α- and β-positions were the first peroxygenation reactions described for P450s being activated directly by H_2O_2. These P450s were $P450_{SP\alpha}$ (Matsunaga et al., 1994), $P450_{BS\beta}$ (Matsunaga et al., 1999) and $P450_{CLA}$ (Girhard et al., 2007). While the former hydroxylated regioselectively (>99%) fatty acids such as myristic and palmitic acid in α-position (**20**), the last two formed a mixture of α- and β-hydroxyderivatives (**20** and **21**). Artificial H_2O_2-dependent P450s were also constructed replacing the Phe87 of $P450_{BM3}$ with an Ala or Gly (Li et al., 2001). These variants successfully catalyzed myristic acid hydroxylation in the presence of H_2O_2, although the turnovers achieved were lower than those of the natural P450-peroxygenases $P450_{SP\alpha}$ and $P450_{BS\beta}$. This α-hydroxylation activity on fatty acids was also found with *Mro*UPO which led to alkyl chain shortening (Olmedo et al., 2017). Indeed, *Mro*UPO was shown to catalyze the progressive one-carbon shortening of medium and long chain mono- and dicarboxylic acids by itself alone, in the presence of H_2O_2. The mechanism starts with an α-oxidation generating an α-hydroxy acid, which is further oxidized by the enzyme to a reactive α-keto intermediate whose decarboxylation yields the one-carbon shorter fatty acid. Concerning fatty alcohol oxygenation (**22**), the above three UPO enzymes oxidize the alcohol to the carboxylic acid as the main product (**23**). In the case of *Aae*UPO and r*Cci*UPO, smaller amounts of both ω-1 (**24**) and ω-2 (**25**) diols were also observed.

In the same way, reactive epoxides derived from unsaturated fatty acids are of industrial interest and have been employed for the synthesis of chemicals and intermediates. Concerning unsaturated fatty-acid oxygenation by UPOs, it has been recently demonstrated that *Mro*UPO, *Cgl*UPO and r*Hin*UPO catalyze the epoxidation of free fatty acids and their methyl esters with high selectivity although some significant differences were observed between enzymes and substrates with the best results in terms of epoxidation selectivity being obtained with the *Cgl*UPO (Aranda et al., 2018c; González-Benjumea et al., 2021). On the other hand, r*Hin*UPO, in addition to forming mono and diepoxides of oleic and linoleic acid (and their methyl esters), respectively, like the other two UPOs, was capable of yielding the triepoxides of α-linolenic acid and its methyl ester (González-Benjumea et al., 2021). In oleic acid (**26**) reactions, UPOs with wider channels (*e.g. Cgl*UPO and *Mro*UPO)

Table 2
Fatty-acid and fatty-alcohol oxygenations by UPOs and some P450s.

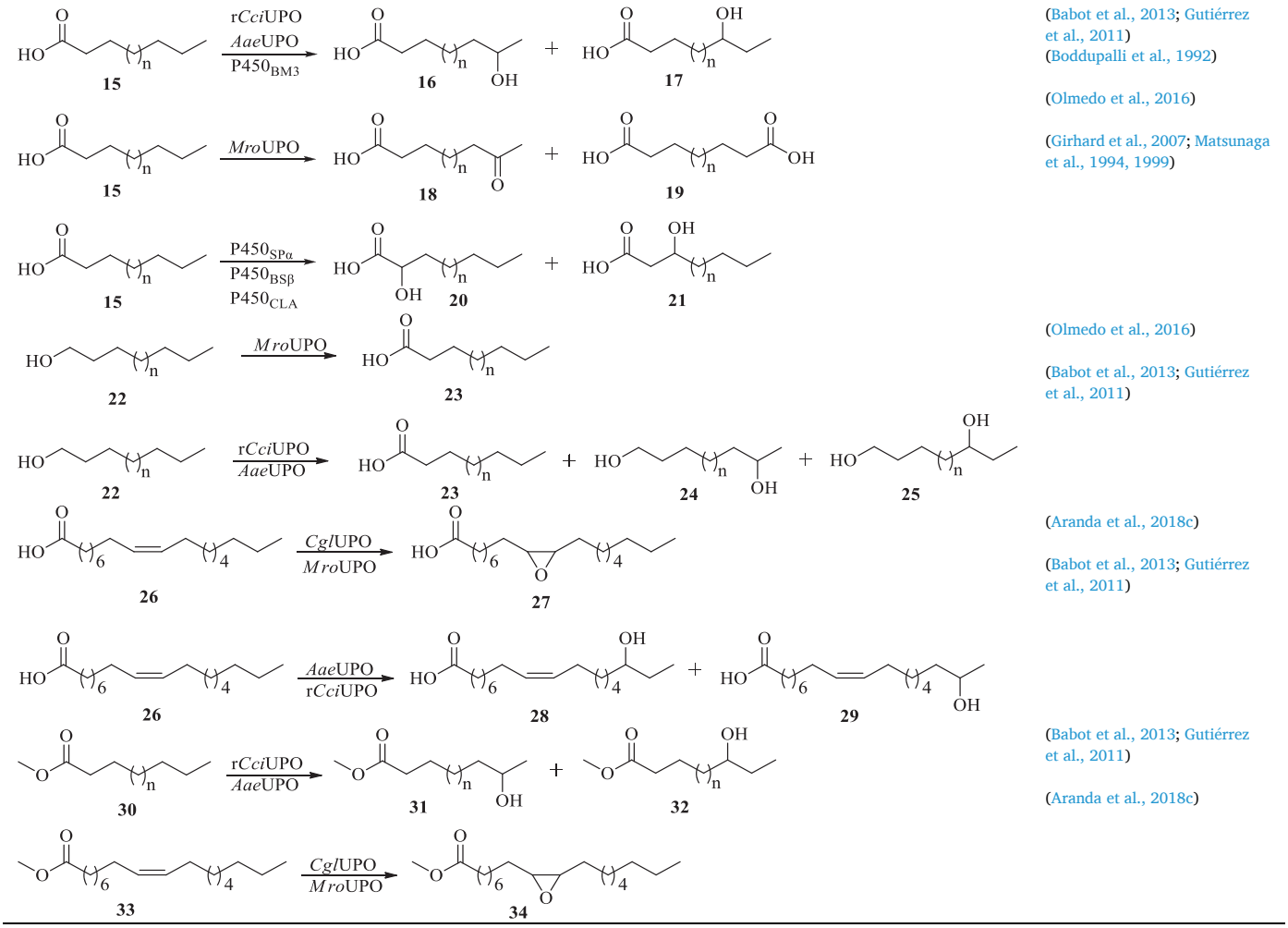

(Babot et al., 2013; Gutiérrez et al., 2011)
(Boddupalli et al., 1992)

(Olmedo et al., 2016)

(Girhard et al., 2007; Matsunaga et al., 1994, 1999)

(Olmedo et al., 2016)

(Babot et al., 2013; Gutiérrez et al., 2011)

(Aranda et al., 2018c)

(Babot et al., 2013; Gutiérrez et al., 2011)

(Babot et al., 2013; Gutiérrez et al., 2011)

(Aranda et al., 2018c)

were shown to epoxidize it (**27**) while the selectivity for the UPOs with narrower channels (*e.g.* r*Cci*UPO and *Aae*UPO) was the same than for saturated fatty acids, hydroxylating oleic acid at subterminal positions (**28** and **29**). Lower selectivity was observed by $P450_{BM3}$, where both in-chain hydroxylation and epoxidation at the double bond were found (Miura and Fulco, 1975) while using *Cgl*UPO high activity and selectivity (>91% in C14:1-C18:1 and C18:2) for epoxidation was observed (Aranda et al., 2018c). Moreover, the main advantage of UPOs over P450s in lipid oxygenation is that while UPOs form the (ω-1) and (ω-2) hydroxy derivatives (**31** and **32**, respectively) of saturated (**30**) and the epoxy derivatives (**34**) of unsaturated (**33**) fatty acids, both in their free and esterified forms, P450s did not transform esterified fatty acids since they seem to need the carboxylic group free for substrate fixation in the heme channel (Miura and Fulco, 1975).

3.3. Alkane and alkene oxygenation

Several examples of oxygenations of alkanes and alkenes by UPOs and some P450s are shown in Table 3. Selective enzymatic oxygenation of alkanes is of high interest since it remains a challenging reaction in organic chemistry, due to the inertness of their C—H bonds. UPOs have been reported to catalyze the selective hydroxylation of linear (C3-C16) alkanes with different regioselectivity depending on the UPO used (Babot et al., 2013; Gutiérrez et al., 2011; Peter et al., 2011). *Aae*UPO and r*Cci*UPO were shown to catalyze the hydroxylation of linear alkanes (**35**) mainly at subterminal ω-1 (**36**) and ω-2 (**37**) positions, while *Mro*UPO was able to catalyze terminal hydroxylation (about 50% of products) (Olmedo et al., 2016). While the main products were the above mono- and dihydroxylated derivatives in the reaction with *Aae*UPO and r*Cci*UPO, with *Mro*UPO the overoxidized acid (**39**) or ketone (**40**) products prevailed. Interestingly, the regioselectivity of the reaction in the hydroxylation of long-chain alkanes by *Aae*UPO and r*Cci*UPO could be tuned varying the proportion of acetone as co-solvent. With low co-solvent concentration (20%) the main products were dihydroxy and hydroxy-keto derivatives, while at higher acetone concentration (40–60%) the mono-hydroxylated derivatives predominated, probably due to higher substrate solubilization (Babot et al., 2013).

Cyclic alkanes (C5-C8) have also been successfully oxygenated by UPOs (Peter et al., 2014) and engineered $P450_{BM3}$ (Pennec et al., 2015). In the selectivity of these reactions it is remarkable that $P450_{BM3}$ variants produced the monohydroxylated derivative, while the UPOs were able to overoxidize the alcohol to ketone, as observed during the oxidation of cyclohexane (**41**) to cyclohexanol (**42**) or cyclohexanone (**43**), with the ketone being more efficiently produced by *Mro*UPO.

Hydroxylation of linear (**35**) and cyclic (**41**) alkanes by P450s has also been extensively studied (Chen et al., 2012; Lentz et al., 2006; Meinhold et al., 2006; Pennec et al., 2015; Weber et al., 2011). For example, up to 92% selectivity in 2-octanol synthesis with the F87V/A328F variant of $P450_{BM3}$ has been obtained from the corresponding alkane (Weber et al., 2011). However, the highest selectivity of P450 variants hydroxylating the most unreactive terminal position of octane to the 1-octanol bulk chemical, was of only 48–52%. Therefore, chimeric

Table 3
Alkane and alkene oxygenations by UPOs and some P450s.

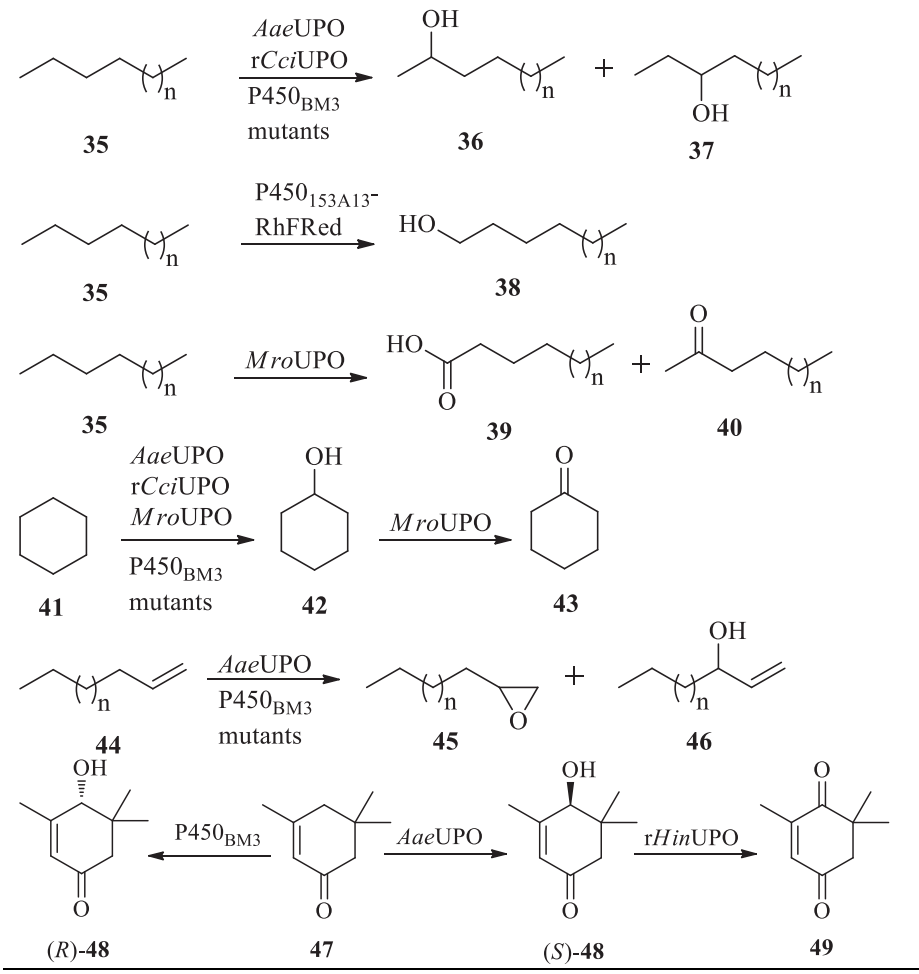

(Babot et al., 2013; Gutiérrez et al., 2011; Peter et al., 2011)
(Pennec et al., 2015)
(Olmedo et al., 2016)

(Peter et al., 2014)
(Pennec et al., 2015)

(Kubo et al., 2006; Peter et al., 2013)

(Aranda et al., 2018b; Peter et al., 2013)

proteins have been constructed fusing P450 domains from the CYP153 family with the reductase domain of $P450_{RhF}$ for the terminal hydroxylation of C6-C8 alkanes (**38**) (Kubota et al., 2005). The comparison of alkane hydroxylation by Pennec et al. (2015) shows how the 2-alcohols could be more selectively (>75%) synthesized using $P450_{BM3}$ variants, while for the synthesis of 1-alcohols the chimeric $P450_{153A13}$-RhFRed enzyme, fusing a P450 domain with the reductase domain of $P450_{RhF}$, was the most selective (>99%) biocatalyst.

Concerning linear (C3-C8, **44**) alkenes, hydroxylation at the allylic position (**46**) has been reported besides double-bond epoxidation **(45)** by both UPOs and P450s (Kaluzna et al., 2016; Kubo et al., 2006; Peter et al., 2013). One interesting example of allylic hydroxylation of a cyclic (C6, **47**) alkene is the synthesis of the flavor-and-fragrance 4-hydroxy and 4-keto derivatives of isophorone. Using $P450_{BM3}$ high regioselectivity and enantioselectivity (>98% and > 99%, respectively) were achieved in the synthesis of (*R*)-4-hydroxyisophorone ((*R*)-**48**), in a system that proved to work at kilogram scale (Kaluzna et al., 2016). Using UPOs, the highest regioselectivity (92%) was achieved with *Cgl*UPO towards the formation of 4-hydroxyisophorone while the highest enantioselectivity (88% *ee*) was attained by *Aae*UPO towards the formation of the enantiomer ((*S*)-**48**) (Aranda et al., 2018b) opposite to that of $P450_{BM3}$. In addition, the 4-ketoisophorone derivative (**49**) can be more efficiently produced by r*Hin*UPO. These UPO conversions of isophorone would be of interest for the flavor-and-fragrance and other industrial sectors (Aranda et al., 2018a).

3.4. Terpene oxygenation

Several examples of small terpene oxygenations by UPOs and some P450s are outlined in Table 4. Small terpenes and their oxygenated derivatives have been the object of study of the flavor-and-fragrance industry from the biological synthesis of compounds such as nootkatone, menthol, citronellol and geraniol (Vandamme and Soetaert, 2002) to the production of hydroxy derivatives for increasing the odor-lasting time of molecules like ionones or isophorone (Serra and De Simeis, 2019). The keto derivative of the latter compound is also used as building block for the synthesis of pharmaceuticals, vitamins and natural pigments (Eggersdorfer et al., 2012; Isler et al., 1956). UPOs have been shown to transform limonene (**50**) epoxidizing both double bonds in 85% and 76% to form the 1,2- and 8,9-epoxides (**51** and **52**), respectively (Peter et al., 2013). In addition, smaller amounts of the hydroxylated derivative at the allylic position, carveol (**53**), were also produced. In the same way, the WT $P450_{BM3}$ also formed (*4R*)-limonene epoxides (37%) and carveol (9%) but in this case the main product was isopiperitenol (54%) with the hydroxyl group at the other allylic position. Interestingly, the regioselectivity of this enzyme could be completely tuned towards terminal methyl hydroxylation to produce perillyl alcohol (**54**), a molecule whose anticancer activities are under extensive studies and clinical trials. While the terminal hydroxylation was not observed in the WT $P450_{BM3}$, after 3 rounds of modeling, design and screening, a triple variant with 97% selectivity towards perillyl alcohol formation could be obtained (Seifert et al., 2011).

Very recently, α- and β-ionone oxygenation by several UPOs

Table 4
Small terpene oxygenations by UPOs and some P450s.

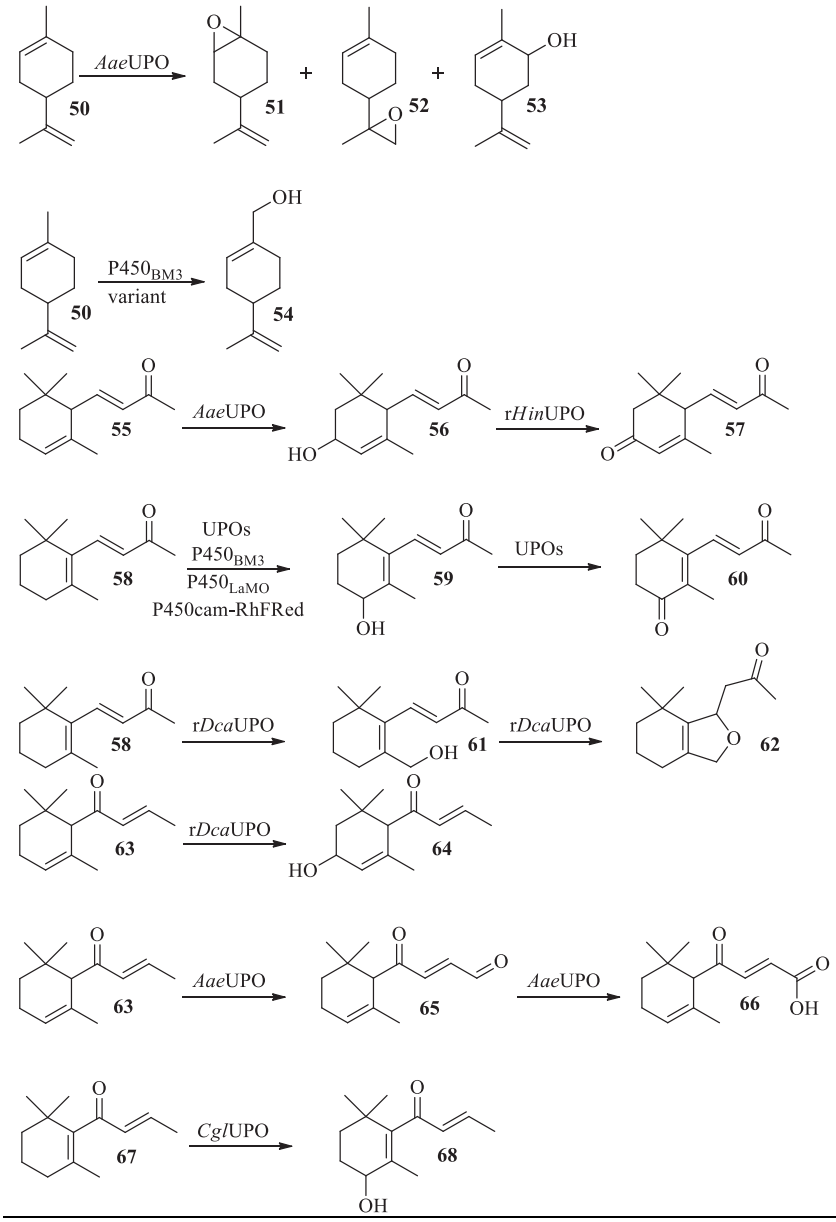

(Peter et al., 2013)
(Seifert et al., 2011)

(Babot et al., 2020)
(Urlacher et al., 2006)
(Yin et al., 2014)
(Robin et al., 2011)

(Babot et al., 2020)

—namely *Aae*UPO, *Mro*UPO, *Cgl*UPO, r*Cci*UPO, r*Hin*UPO and r*Dca*UPO— has been reported (Babot et al., 2020). Both ionones were completely transformed (>99%) by most UPOs (in 5–30 min reactions with up to 6,200 TTN). In the case of α-ionone (**55**), the highest selectivity was achieved with *Aae*UPO and r*Hin*UPO forming 3-hydroxy-α-ionone (**56**) and 3-keto-α-ionone (**57**) with 93% and 98% regioselectivity, respectively. β-Ionone (**58**) was mostly hydroxylated at the cyclohexene allylic position to form 4-hydroxy-β-ionone (**59**), again with the highest selectivity (87%) attained by *Aae*UPO. Other UPOs (*Mro*UPO, *Cgl*UPO and r*Hin*UPO) overoxidized this compound into 4-keto-β-ionone (**60**). Interestingly, r*Dca*UPO was the only UPO able to hydroxylate the β-ionone C-13 position yielding **61**, whose subsequent cyclation yielded 7,11-epoxymegastigma-5(6)-en-9-one (**62**, 11% of products), in a reaction not reported for P450s or microbial cultures so far. Moreover, the structurally similar α- and β-damascones (**63** and **67**, respectively), with the keto group and double bond of the side chain exchanged with respect to the corresponding ionones, were also tested as substrate of UPOs (Babot et al., 2020). The selectivity towards these compounds was similar to that observed with ionones, with the oxygenated derivatives in the allylic position as the main reaction products, and *Aae*UPO being able to oxygenate the terminal position of the side chain. Remarkable selectivities were achieved by *Aae*UPO and r*Dca*UPO, respectively, towards formation of the carboxylic (**66**, 80%) and 3-hydroxy (**64**, 83%) derivatives of α-damascone (the former *via* the aldehyde intermediate, **65**), and the one obtained by *Cgl*UPO in the formation of 4-hydroxy-β-damascone (**68**, 88%).

Selective hydroxylation of ionones by P450s has also been studied (Robin et al., 2011; Urlacher et al., 2006; Yin et al., 2014). While WT $P450_{BM3}$ showed low activity with β-ionone (**58**), it could be increased up to 300-fold after site-directed mutagenesis and two rounds of error-prone PCR. Contrary to UPOs, the $P450_{BM3}$ variants selectively produced only 4-hydroxy-β-ionone (**59**) while the selectivity decreased with α-ionone forming a mixture of four oxygenated products. The same was observed with $P450_{LaMO}$, hydroxylating selectively β-ionone at the C-4 position, while oxidizing α-ionone in four different positions (Yin et al., 2014). In addition, mutated variants of the chimeric $P450_{cam}$-RhFRed

protein also showed activity towards α- and β-ionone attaining complete conversion (>99%) and regioselectivity of both substrates (Robin et al., 2011).

3.5. Steroid oxygenation

Representative examples of oxygenation reactions of steroids by UPOs and some P450s are outlined in Table 5. Steroids are a good example of how hydroxylation strongly affects (usually increasing) the biological activity. In addition, the position where the hydroxyl group is located also influences the activity. For example, the hydroxyl at position 11β is essential for anti-inflammatory activity of steroids such as cortisol or prednisolone (Fegan et al., 2008). The position of the hydroxyl group in the side chain of steroids is also relevant as, for example, the 25-hydroxy functionality in the cholesterol derivative confers its antiviral activity (Blanc et al., 2013; Liu et al., 2013) and the 25-hydroxyderivative of the secosteroids vitamin D2 and D3 showed better properties in the treatment of several diseases (Buck et al., 2013; Jean et al., 2008; Jones, 2013). Moreover, other oxygenation reactions such as epoxidations also produce interesting derivatives involved in the regulation of cell proliferation and cholesterol homeostasis (Murphy and Johnson, 2008).

Among reactions catalyzed on steroids, testosterone (**69**) hydroxylation has drawn interest for the application of P450s. WT $P450_{BM3}$ was unable to oxygenate testosterone and directed evolution was needed to achieve substrate transformation. The first variants afforded were able to oxygenate positions 2 and 15 with high stereoselectivity and substrate conversion (Bureik and Bernhardt, 2007; Kille et al., 2011), but the final target was position 16 due to the value of the alcohol formed as component of biologically-active glucocorticoids (Bureik and Bernhardt, 2007). In a first attempt, Commandeur and co-workers engineered $P450_{BM3}$ variants for testosterone 16-hydroxylation (with 60–85% selectivity) at expenses of lower enzyme activity and substrate conversion (Rea et al., 2012; Venkataraman et al., 2012; Vottero et al., 2011). Some years later, using an improved directed evolution strategy, the desired 16-hydroxylation of testosterone (yielding α-**70** and β-**70**) was

Table 5
Steroids oxygenations by UPOs and some P450s.

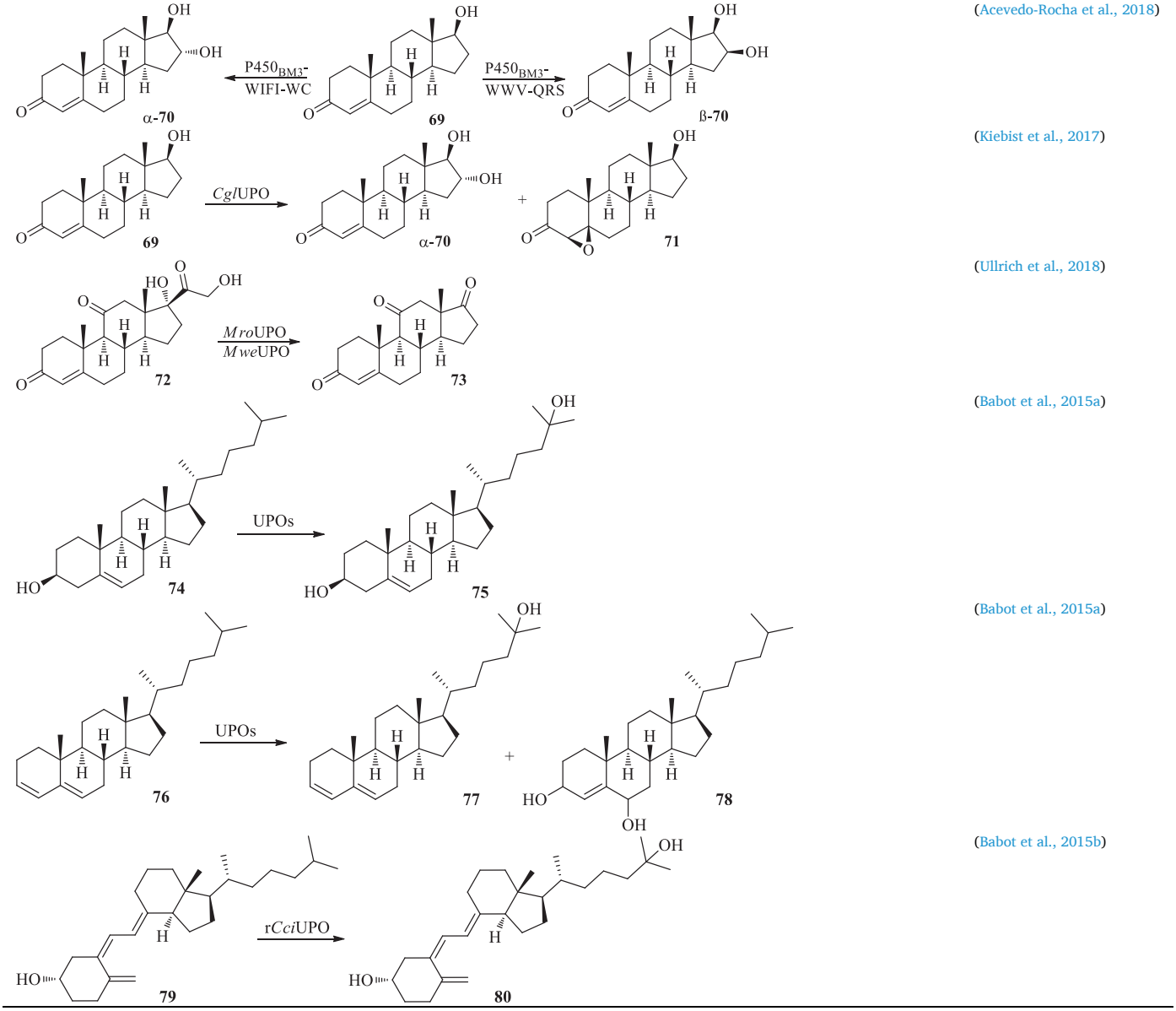

(Acevedo-Rocha et al., 2018)

(Kiebist et al., 2017)

(Ullrich et al., 2018)

(Babot et al., 2015a)

(Babot et al., 2015a)

(Babot et al., 2015b)

reported with higher selectivity (72–100%) and conversion (59–99%) (Acevedo-Rocha et al., 2018). Moreover, the two enantiomers from four additional steroids —androstenedione, nandrolone, boldenone and norethindrone— were in most cases accessible with stereo-complementary biocatalysts. Among UPOs, only *Cgl*UPO has been reported to transform testosterone (**69**) producing mainly the epoxide (**71**, 90%) and minor amounts of α-**70** derivatives (Kiebist et al., 2017). Transformation of methyltestosterone in addition to testosterone has also been reported for $P450_{BM3}$ variants (Liu et al., 2016a). Interestingly, when corticosteroids have both hydroxyl (like testosterone) and hydroxyacetyl functionalities at C-17 (**72**), *Mro*UPO is able to catalyze the side-chain removal of these molecules (**73**) (Ullrich et al., 2018).

On the other hand, the regioselective hydroxylation of several steroids differing in their structures, including free and esterified sterols and steroid ketones and hydrocarbons, were reported for *Aae*UPO, *Mro*UPO and r*Cci*UPO by Babot et al. (2015a). Hydroxylation at the side chain over the steroidal rings was preferred, with the 25-hydroxyderivatives predominating (with regioselectivities >99% in most cases) as in the case of cholesterol (**74**) yielding 25-hydroxycholesterol (**75**). However, hydroxylation at the ring moiety and terminal hydroxylation at the side chain also was observed in some steroids, the former favored by the absence of oxygenated groups at C-3 and by the presence of conjugated double bonds in the rings as in the case of cholesta-3,5-diene (**76**) which yielded 25-hydroxycholesta-3,5-diene (**77**) and 3,6-dihydroxycholest-4-ene (**78**).

Another interesting example of this side-chain reactions by UPO is the hydroxylation of the secosteroid vitamin D (**79**) in C-25 to form the active hydroxylated metabolite (**80**) with >99% regioselectivity (Babot et al., 2015b).

4. Enzyme engineering

4.1. Heterologous expression and directed evolution

The heterologous expression of proteins, which enables the obtention of an enzyme from an organism other than its natural producer, is of paramount importance for enzymology application. The organisms that naturally produce a given enzyme often require special culturing and specific inductive conditions (Lambertz et al., 2014), which can be difficult to provide in the laboratory. In contrast, the organisms employed as heterologous producers are well-characterized, and a wealth of techniques that allow their genetic manipulation for the study of enzyme mechanisms and the creation of mutated variants are nowadays available (Bill, 2014). Moreover, they offer higher expression levels for their applicability to industrial processes, and facilitate protein crystallization to unveil the structural determinants of catalysis, as commented below. In fact, the heterologous expression methods paved the way for the studies on structure-function of P450, which were formerly impaired due to the animal and human origin of most of them (Guengerich et al., 2016). Moreover, with the advent of systems biology, the heterologous expression allows creating chemical factories using fermentable organisms and to assembly pathways implicating enzymes of diverse origins in a same heterologous host (Wei et al., 2018).

First published attempts to engineer UPOs started with directed evolution of *Aae*UPO towards its functional expression in *Saccharomyces cerevisiae*, attaining 27-fold improved UPO production after evolution of its signal peptide (González-Pérez et al., 2014). Additional rounds of directed evolution on the *Aae*UPO gene, brought about a further 1000-fold improvement of protein expression as well as an enhancement in the biochemical properties of the enzyme —specific activity and co-solvent stability— that made it more suitable for application (Molina-Espeja et al., 2014). Moreover, the mutated variant obtained (PaDa-I) was transferred for expression in a tandem-yeast expression system composed of *S. cerevisiae* and *K. pastoris*, which benefits from the ease of genetic manipulation of the former and the high expression levels of the latter (Molina-Espeja et al., 2015a). Genetic drift and *in vivo* DNA shuffling of the *Aae*UPO gene has also been employed to improve thermostability, co-solvent stability, as well as broadening the promiscuity of the enzyme with success (Martín-Díaz et al., 2018). The above studies resulted in several patents for the industrial production and use of evolved *Aae*UPO (Gómez de Santos et al., 2018; Molina-Espeja et al., 2015b). Very recently, first-time expression of four UPO genes —of the already mentioned *Mro*UPO and *Cgl*UPO, together with UPOs of *Myceliophthora thermophila* (*Mth*UPO) and *Thielavia terrestris* (*Tte*UPO)— in yeast hosts (*S. cerevisiae* and *K. pastoris*), without a previous directed-evolution adaptation of their nucleotide sequences, has been reported using a modular secretion system (Püllmann et al., 2020). In addition to yeast production of *Aae*UPO, other UPO enzymes (such as *Coprinopsis cinerea* and *Humicola insolens* UPOs) have also been heterologously produced in eukaryotic expression hosts, such as *Aspergillus oryzae* by Novozymes A/S (Bargsvaerd, Denmark), and used in different applications (Babot et al., 2013; Kiebist et al., 2017), although the details on their heterologous production by this company are not publicly available.

Although fungi, such as *Aspergillus* species and *K. pastoris*, are the election hosts for large-scale production of UPO enzymes, *Escherichia coli* expression is in general preferred for structure-function studies and enzyme engineering. Unfortunately, all attempts to activate UPO *in vitro* after its over-expression as bacterial inclusion bodies, a production strategy widely used with different heme peroxidases (Fernández-Fueyo et al., 2014; Linde et al., 2014; Miki et al., 2009; Pérez-Boada et al., 2002), were unsuccessful with UPOs. However, recently UPO expression in *E. coli* as soluble and active enzymes has been reported (Carro et al., 2019; Fernández-Fueyo et al., 2018; Linde et al., 2020), and applied to rational design of these enzymes, as described below.

4.2. Molecular structure and heme-thiolate active site

The first reports on UPO rational design have been very recently brought to light, after solving the first UPO crystal structures. So far, only the crystal structures of wild (Piontek et al., 2010, 2013) and evolved (Ramírez-Escudero et al., 2018) *Aae*UPO, and of wild *Mro*UPO are available, with PDB accession numbers including 2YP1, 5OXU and 5FUJ, respectively. The latter structure, however, lacks a specific associated publication, although it has been used in different studies (Aranda et al., 2018b and 2018d; Carro et al., 2019). Although they belong to two different UPO families (Hofrichter et al., 2015), the so-called long (family II) and short (family I) UPOs, respectively, they do share a number of general features. At first glance one can observe that their secondary structures are predominantly helicoidal: both of them bear ten α-helices along with very short β-strands, five in *Aae*UPO and two in *Mro*UPO (**Fig. 4A** and **B**, respectively). All UPOs contain an iron protoporphyrin IX as a prosthetic group, which is bound to an exposed cysteine (*Aae*UPO Cys36 and *Mro*UPO Cys17) located on its lower axial side (also known as proximal side because it contains the above proximal residue acting as iron ligand), hence their classification as heme-thiolate proteins. To ensure that the sulfhydryl moiety of such cysteine is exposed towards the heme iron, of which it acts as the 5th coordinating ligand, virtually all UPO sequences share the so-called PCP motif (Hofrichter et al., 2015). Moreover, UPO catalysis (activation by H_2O_2 step) involves the presence of an acid-base pair at the upper side (also known as distal side) of the heme group, represented by a glutamate residue (*Aae*UPO Glu196 and *Mro*UO Glu157) in the vicinity of a basic arginine or histidine residue (*Aae*UPO Arg189 and *Mro*UO His86) in long and short UPOs, respectively. Another structural similarity is the presence of a Mg^{2+} ion, which was identified by ICP-MS in the *Aae*UPO structure, tetracoordinated with the carboxylate and hydroxyl groups of the heme propionate and the side chains of three aspartate, glutamate and serine residues (Piontek et al., 2010). It is likely that this cation contributes to the cofactor binding at the heme pocket. Both enzymes are also glycosylated: *Aae*UPO contains around 20% glycosylation of the high mannose type (Pecyna et al., 2009; Piontek et al., 2013), whereas

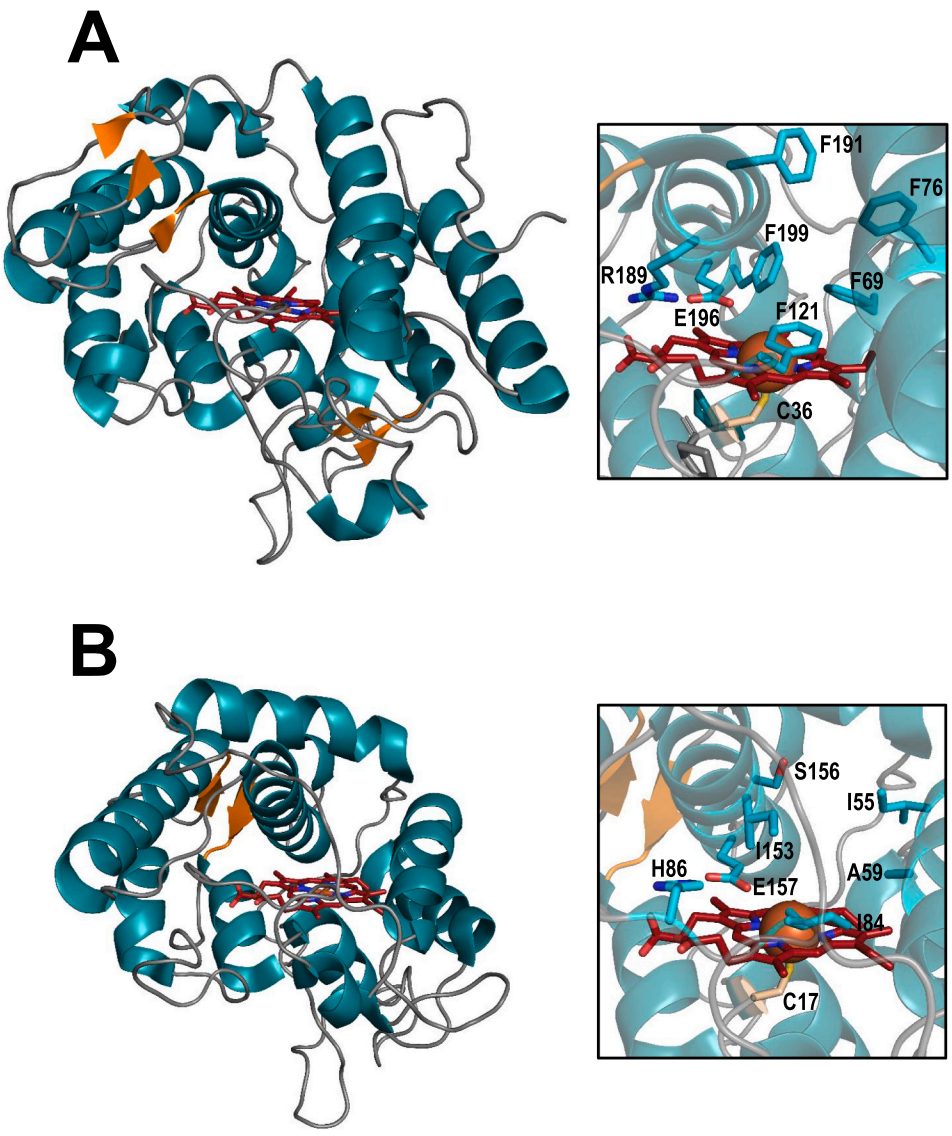

Fig. 4. Scheme from crystal structures of *Aae*UPO (**A**) and *Mro*UPO (**B**), with details of their heme regions (right insets), from PDB entries 2YP1 and 5FUJ, respectively. Ribbon-like representation with 10 helices in blue, very short β-structures in orange, heme and neighbor residues as CPK-colored sticks, and iron cation as van der Waals sphere. (For interpretation of the references to colour in this figure legend, the reader is referred to the web version of this article.)

the 16% of the mass of *Mro*UPO would correspond to carbohydrates (Gröbe et al., 2011).

In spite of the above homologies, there exist notable differences between the two UPO types concerning their sizes and quaternary structure. While wild *Aae*UPO weighs around 46 kDa (Ullrich et al., 2004), the wild *Mro*UPO is of around 32 kDa (Gröbe et al., 2011). Apart from the likely differences in glycosylation that may affect the molecular weight of the proteins, such difference is mainly due to the length of their amino-acidic sequences. In fact, the full *Aae*UPO sequence contains 353 amino acids (Pecyna et al., 2009) —of which only 325 appear in the crystal structure after signal peptide cleavage— (Piontek et al., 2013), whereas the crystal structure of *Mro*UPO (belonging to the short-UPO family) only includes 234 amino acids after loss of a 30-residue signal peptide. Regarding quaternary structure, whereas the enzyme from *A. aegerita* is secreted as a monomer, the one from *M. rotula* is found as a homodimer, as revealed by the molecular masses estimated by native HPLC-SEC under native conditions (62 kDa) and SDS-PAGE under denaturing conditions (32.5 kDa) (Ullrich et al., 2018). The same appears to be true for other members of the UPO families I and II (Hofrichter et al., 2020). The dimeric nature of *Mro*UPO is maintained through an intermolecular disulfide bridge between Cys227 at the *C*-terminal region of each monomer (Olmedo et al., 2017), as well as other interactions between the *C*-termini, as revealed by the crystal structure. On the other hand, monomeric *Aae*UPO also possesses an intramolecular disulfide bridge (between Cys278 and Cys319) that is thought to render its *C*-terminal region more stable (Piontek et al., 2013).

Additional dissimilarities between the above UPOs arise upon closer inspection of their active sites, located at the upper side of the heme group, where interactions with both the oxidizing and reducing substrates take place. That of *Aae*UPO bears a resemblance with the shape of an inverted frustum, the heme group is buried at around 17 Å from the solvent and has external and internal widths of 10 and 8.5 Å, respectively (Piontek et al., 2013). On the contrary, the active site —and the channel connecting it to the solvent— seem to be bigger in the case of *Mro*UPO. Another difference that strongly affects the substrate scope is the type of residues upholstering the heme channel and the active site of each of these model enzymes. While *Aae*UPO possesses aromatic residues lining the cavity and the channel, including up to five phenylalanines, some of which act as a sort of "clamp" that restricts the position of the substrate over the heme cofactor, *Mro*UPO bears ten aliphatic

(leucine and isoleucine) residues. The chemical nature of such amino acids seems to determine the substrate preference of each type of enzyme: whereas *Aae*UPO displays preference towards aromatic substrates (Aranda et al., 2009; Karich et al., 2013; Kluge et al., 2009, 2012; Ullrich et al., 2008), *Mro*UPO tends to be active towards larger aliphatic molecules (Babot et al., 2015a; Olmedo et al., 2017; Ullrich et al., 2018) including fatty acids (Carro et al., 2019; Olmedo et al., 2017).

4.3. Computationally-aided enzyme rational design

On the basis of the UPO crystal structures mentioned above, and some homology molecular models (*e.g.* of r*Cci*UPO showing 55% sequence identity with *Aae*UPO), computational simulations of substrate diffusion and accommodation at the enzyme active site have been performed. Those employed the PELE software for dynamic ligand diffusion in proteins (Lecina et al., 2017), together with molecular dynamics. The computational analyses had a double purpose: **i)** To rationalize the observed different UPO activities; and **ii)** To propose amino-acid substitutions in the active-site (and other protein regions) for rational design towards target reactions.

One of the first examples of the former approach was the study on steroid hydroxylation by UPOs. Simulations revealed that the active-site geometry and hydrophobicity favor the entrance of the steroid side chain to different extents, while the entrance of the ring is energetically penalized, in agreement with the experimental reaction yields obtained (Babot et al., 2015a). Similar PELE simulations explained the selective hydroxylation of cholecalciferol (vitamin D_3) and ergocalciferol (vitamin D_2) by r*Cci*UPO, yielding the bioactive C_{25}-OH derivatives (Lucas et al., 2016). The calculations revealed that differences in the access-channel resulted in the perfect substrate fitting on r*Cci*UPO, while the broader *Aae*UPO channel (Fig. 5) permits a variety of substrate poses and reactivities. PELE computational simulations also elucidated the selectivity of two ascomycete UPOs (*Cgl*UPO and r*Hin*UPO) hydroxylating isophorone to its 4-OH and 4-oxo derivatives, compared with three basidiomycete UPOs (*Aae*UPO, r*Cci*UPO and *Mro*UPO) whose active sites do not accommodate isophorone and 4-hydroxyisophorone at the required position for C_4-hydroxylation (Aranda et al., 2018b).

Given the current interest in vegetable oils as renewable raw materials for a bio-based chemical industry, UPO rational design has focused on improving the selectivity of these enzymes towards the epoxidation of unsaturated fatty acids to yield reactive epoxides. Such studies have been facilitated by the availability of the convenient *E. coli* expression system for protein engineering mentioned above, and are also taking advantage of the available molecular structures and the reaction predictions provided by computational simulations. Rational design started with *Mro*UPO (Carro et al., 2019), since this was the first UPO expressed in *E. coli* as an active enzyme, being more recently continued with *Cvi*UPO (González-Benjumea et al., 2020) due to the higher yields and easier isolation of this recombinant enzyme (Linde et al., 2020). Results from simulated diffusion and accommodation of oleic acid at the *Mro*UPO active site identified key residues whose directed mutagenesis enabled to modulate the hydroxylation *vs* epoxidation activity of this enzyme. According to the results, mutations were suggested that widen the heme access channel and that should promote oleic acid approach in a bent configuration (Fig. 6A), enabling its effective epoxidation by oxygen transfer from the neighboring $Fe^{4+}=O$ of the peroxide-activated UPO. Conversely, introduction of bulky residues would only permit oleic acid to enter the UPO channel in an extended configuration (Fig. 6B) resulting in subterminal hydroxylation, without double bond epoxidation. Interestingly, the predicted shift in UPO hydroxylation *vs* epoxidation activity was experimentally confirmed by GC–MS of oleic acid products from reactions with the mutated variants expressed in *E. coli* (**Fig. 6C** and **D**) (Carro et al., 2019). Taking the above results into account, an UPO variant epoxidizing linoleic and α-linolenic acids, but not oleic acid, was obtained by narrowing the heme channel of the *E. coli*-expressed *Cvi*UPO mentioned above (González-Benjumea et al., 2020),

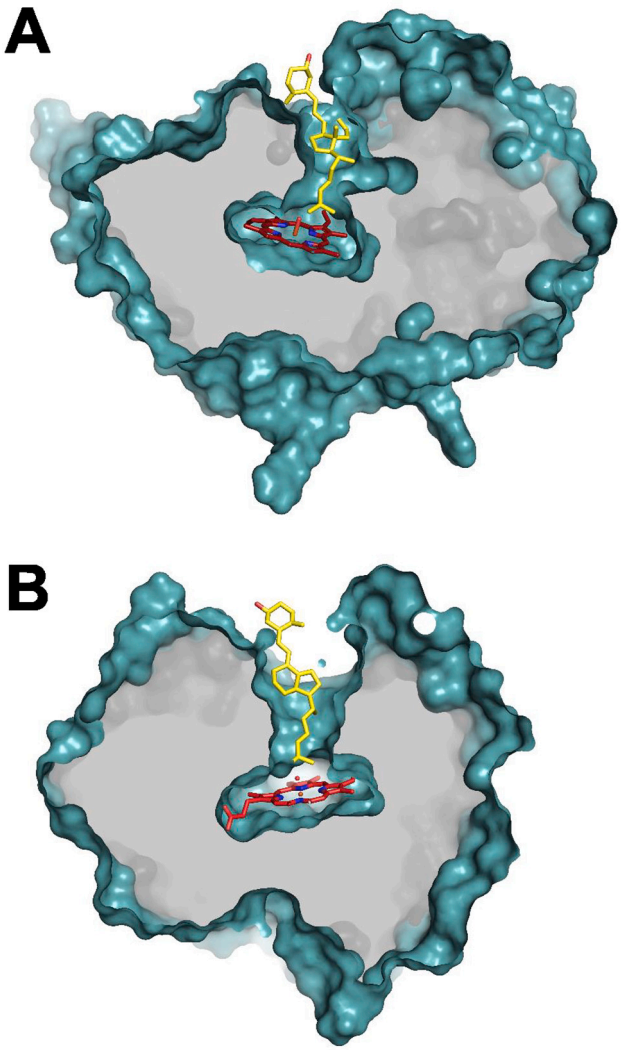

Fig. 5. Perfect fitting of vitamin D_3 inside the heme access-channel of the *C. cinerea* UPO predicted by PELE (**A**), which results in selective hydroxylation at C25 position yielding bioactive 25-hydroxycholecalciferol, compared with its position at the broader channel of *Aae*UPO (**B**), where different side-chain positions are allowed resulting in several hydroxylated products. The solvent-access surface is shown in cyan, and both the substrate and heme molecules, the latter as simulated compound-I, are shown as CPK-colored sticks (yellow and red carbons, respectively). (For interpretation of the references to colour in this figure legend, the reader is referred to the web version of this article.)

whose potential for partial epoxidation of vegetable oil hydrolyzates is being investigated. Very recently, a comprehensive computational and experimental study satisfactorily predicted the reactivity of the above UPOs on different C18 unsaturated fatty-acid substrates, enabling enzyme engineering for regio- and stereo-selective monoepoxidation of α-linolenic acid at preparative scale (Municoy et al., 2020). These and other monoepoxides from polyunsaturated fatty acids are nearly impossible to be obtained by chemical means, and the enzymatic synthesis developed is of high interest given the biological activity of these compounds, in addition to their application in organic synthesis as highly reactive molecules.

4.4. Structural-functional analogies and dissimilarities in P450s

Although they are not phylogenetically related to UPOs, P450s show some common features with them in the sense that they are also heme-thiolate enzymes, which implies that P450s share the same cofactor and

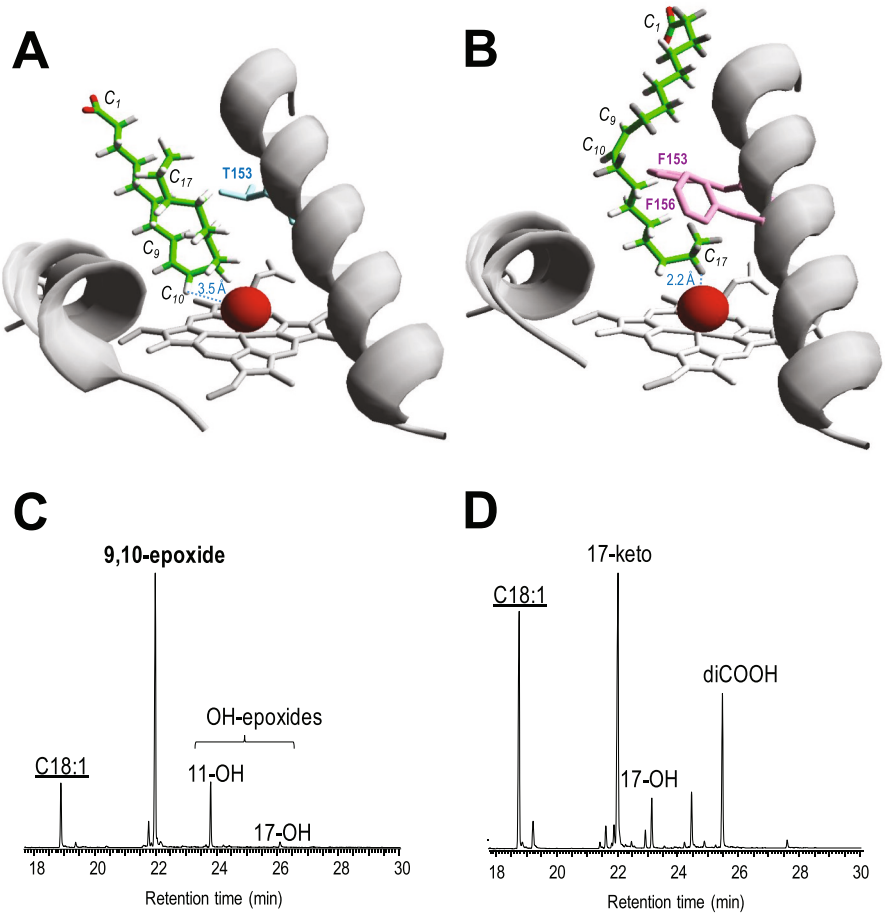

Fig. 6. Docking of oleic acid (18:1 as CPK-colored sticks with carbons in green) on the I153T (**A**) and I153F/S156F (**B**) *in silico* variants of *Mro*UPO (detail of ribbon model) with indication of distances (in Å) between the compound I oxygen atom (red sphere) and the substrate C_{10} (**A**) and C_{17} (**B**) hydrogens, resulting in double-bond epoxidation by the former variant (**C**) and (sub)terminal hydroxylation by the second variant (**D**) as shown by chromatographic analyses. Mutated residues Thr153 (**A**) and Phe153 and Phe156 (**B**) and heme cofactor are shown as cyan, pink and gray sticks, respectively. (For interpretation of the references to colour in this figure legend, the reader is referred to the web version of this article.)

way of binding it to the apoenzyme as UPOs. In this way, P450s possess, albeit with slight variations, a signature sequence FXXGXXXCXG, conforming a β-turn which bears the abovementioned cysteine that acts as the fifth ligand of the heme (Syed and Mashele, 2014). This is also what confers them their unique spectroscopic absorbance properties, displaying a maximum at 450 nm in its cysteine-thiolate form of the ferrous-carbon monoxide complex.

In spite of the fact that P450 sequence identities among families are not high (around 40%), since P450s constitute a vast superfamily of different enzymes of widespread origins, and despite their varying sizes ranging from 350 to 540 amino acids, the overall P450 fold is very conservative (Poulos, 2005), except in the active site, so that they can accommodate a wide variety of substrates (Denisov et al., 2005). In any case, P450s are triangular-shaped and also predominantly helicoidal proteins. Typically, they present 12 α-helices (designated from A to L in alphabetical order from the *N*-terminus), which tend to be conserved, although additional ones may be found, and they also normally bear at least one conserved β-sheet in the *N*-terminal region (Johnson and Stout, 2013). Moreover, three of these helices are highly conserved, which are F, G and, especially, I. F and G constitute a sort of lid that covers the active site and that is mobile to permit the substrate access. It is noteworthy that P450s, unlike UPOs, do not usually display a clearly visible heme access channel connecting the protein surface to the heme cofactor, which is deeply embedded into the protein core (Urban et al., 2018). Helix I is located in the close vicinity of the heme cofactor and has been proposed to bear the O-binding motif, hence its conservation among the superfamily members (Anzenbacher et al., 2008). In fact, a crucial residue for catalysis, a highly conserved threonine, which is involved in the transfer of protons from water molecules to the Fe-oxo species (from the heme reaction with dioxygen) to give rise to compound I so that catalysis can progress, is placed in helix I (Shaik et al., 2005). In this way, concerning their active sites, the majority of P450 enzymes possess an acid-alcohol amino acid pair, constituted by the said threonine and aspartic acid (Girvan et al., 2007). Nevertheless, the latter residues are replaced by arginine and proline, which can bind carboxylates, in several P450 enzymes acting as peroxygenases. These enzymes do not need to transfer the protons from water molecules, since they are reactive with H_2O_2 thanks to the interaction of the arginine with their respective substrate carboxylate groups, which facilitates H_2O_2 activation (Munro et al., 2018). Furthermore, those also bear a longer loop at the proximal side, which would prevent electron transfer, since they do not require redox partners (Fujishiro et al., 2011), the otherwise conserved phenylalanine located 7 residues before the cysteine being absent in these kind of enzymes.

There exists one striking feature of canonical P450s monooxygenases that can be observed on the surface of the enzyme. They normally display a superficial patch of basic and hydrophobic residues in the vicinity of the proximal side of the heme cofactor (Keenaan et al., 2011). It has been considered as a motif where the redox partners bind in order to transfer the electrons to the heme cofactor. P450 peroxygenases also present differences in the surface potential distribution because they do not need to interact with other proteins acting as redox partners (Belcher et al., 2014).

One additional dissimilarity between P450s and UPOs is that the former are often membrane-bound proteins. They are, thus, anchored to membranes through an amphipatic helix located at the N-terminus of the protein. Generally, this enzyme area is immersed in the upper leaflet of the membrane, whereas the catalytic domain tends to be exposed to the solvent (Šrejber et al., 2018). The exception is the soluble P450s with a fused flavin-reductase domain, which act as self-sufficient

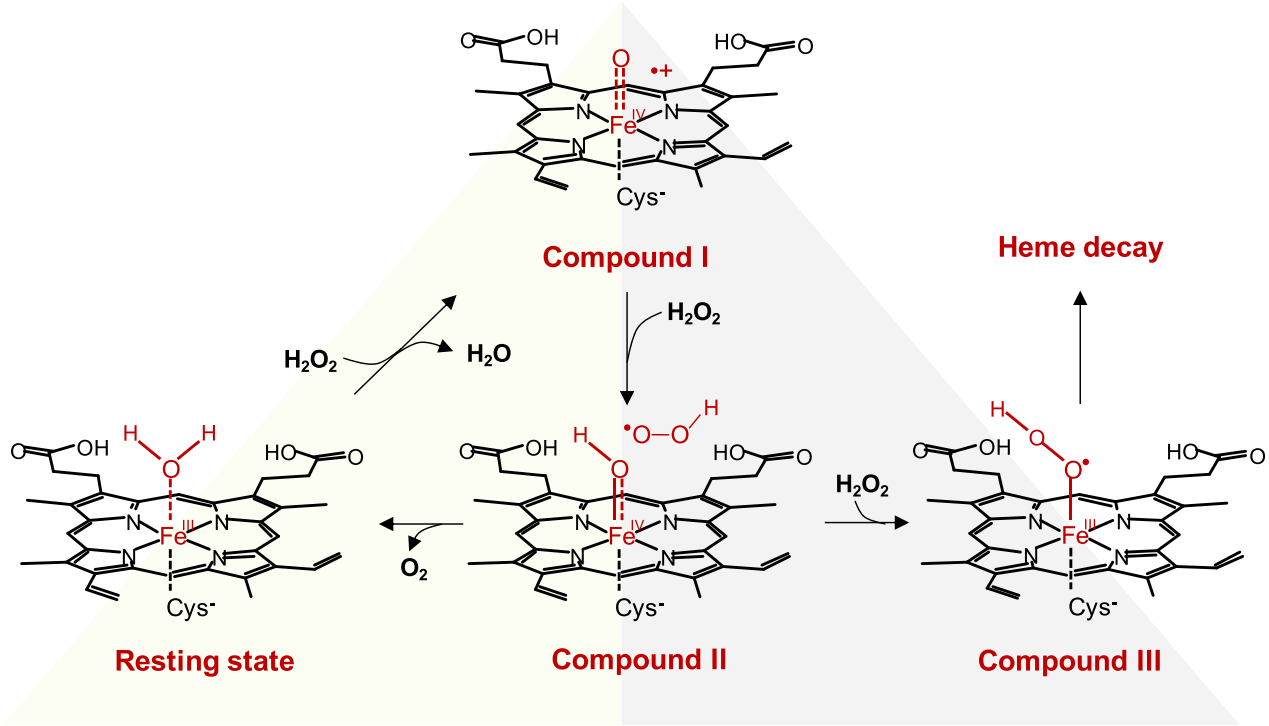

Fig. 7. Scheme of UPO reaction cycle in the presence of peroxide excess, resulting in compound III formation, by non-productive use of peroxide ("catalase-type" activity), and final heme bleaching and decay.

monooxygenases.

Naturally, like UPOs, P450S are also the object of enzyme engineering studies through directed evolution (Behrendorff et al., 2015) and rational design (Xu and Du, 2018). An example of directed evolution studies is illustrated by Acevedo-Rocha et al. (2018). In such work, saturated and iterative saturated mutagenesis is applied to 2 groups of a total of 10 residues lining the active-site pocket, stemming from previous structure-function studies. In this way, the regioselectivity of the enzymes is shifted towards the position C16 of 5 different steroids, obtaining mutants with unusual activity on these compounds. An additional example of rational design on P450s is exemplified by Neufeld et al. (2013) for the hydroxylation of bulky substrates on benzylic C—H bonds. In this case, in the light of previous structural information on catalysis of this kind of substrates, three position of P450 BM3 are selected —87, 51 and 188— to be mutated. The obtained variants were screened for their catalysis on a model substrate, so that double mutant F87A/L188C was found to be especially interesting, since it proved to be useful at small preparative scale for the production of benzylic derivatives, displaying better conversion rates and selectivity than the parental enzyme.

5. Process engineering

Because of their extracellular nature, UPOs are easily applied as isolated biocatalysts in crude extracts or purified forms. In contrast, P450s are intracellular proteins so they need to go through cell lysis procedures before being applied as crude extracts, which are less stable due to their intracellular origin. Even though some P450s are self-sufficient, with the reductase and heme domains fused, they still need expensive cosubstrates (NAD[*P*]H) for catalysis and usually regeneration systems are combined for cofactor recycling, *e.g.* based on glucose oxidation by glucose dehydrogenase. For that reason, P450s are often applied as whole-cell systems, which are cheaper and easier to handle using the internal cofactor regeneration system of cells, although solubility issues and competitive processes inside the cells usually lead to lower yields and selectivities.

Biocatalytic oxyfunctionalization reactions of aliphatic compounds are usually limited by the substrate solubility in water, since enzymatic reactions are usually performed in aqueous buffers, and therefore, high hydrophobic substrates are restricted to low substrate concentration, which is not economically and environmentally feasible. To circumvent this issue, reactions are performed using organic (co)solvents either miscible or immiscible with water in two-liquid-phase systems. In this sense, UPOs have proven to present high stability towards a number of organic solvents such as acetone and acetonitrile in which the full enzyme activity was maintained during at least 2 h in 60% solvent (Peter et al., 2011). In addition, UPOs are also able to work with organic peroxides allowing for the use of high co-solvent proportion or even non-aqueous reaction conditions (Fernández-Fueyo et al., 2016). However, due to the substrate promiscuity of UPOs, it is difficult to find an adequate organic solvent in which to perform reactions in biphasic systems and these has been mostly applied when the organic solvent was the substrate itself (Fernández-Fueyo et al., 2016).

With peroxygenases (UPOs included), a major consideration to take into account for their application is the co-substrate supply. They need peroxides for the catalysis but high concentrations of these oxidants can lead to enzyme inactivation and peroxide destruction, through a compound III formation (Fig. 7) (Kiebist et al., 2017). For that reason, the H_2O_2 supply needs to be thoroughly optimized for each particular reaction since besides different stability to H_2O_2, UPOs also present different extent of the above "catalase activity" depending on the substrate affinity. Therefore, H_2O_2 concentration should be low to avoid enzyme inactivation and peroxide destruction but high enough to achieve maximum velocities and high space-time-yields. To that end, H_2O_2 is usually continuously dosed with pumps or *in situ* generated, avoiding in the last case increase in reaction volumes.

Several enzymatic and chemical methods have been reported to generate the H_2O_2 for UPO-catalyzed reactions (Fig. 8). Most of the enzymatic methods rely on the reductive activation of O_2 to H_2O_2 by oxidases using cosubstrates such as glucose (Kiebist et al., 2017) (Fig. 8A), methanol (Ni et al., 2016) (Fig. 8B) or formate (Tieves et al., 2019) (Fig. 8C) as electron donors, and they have been combined with

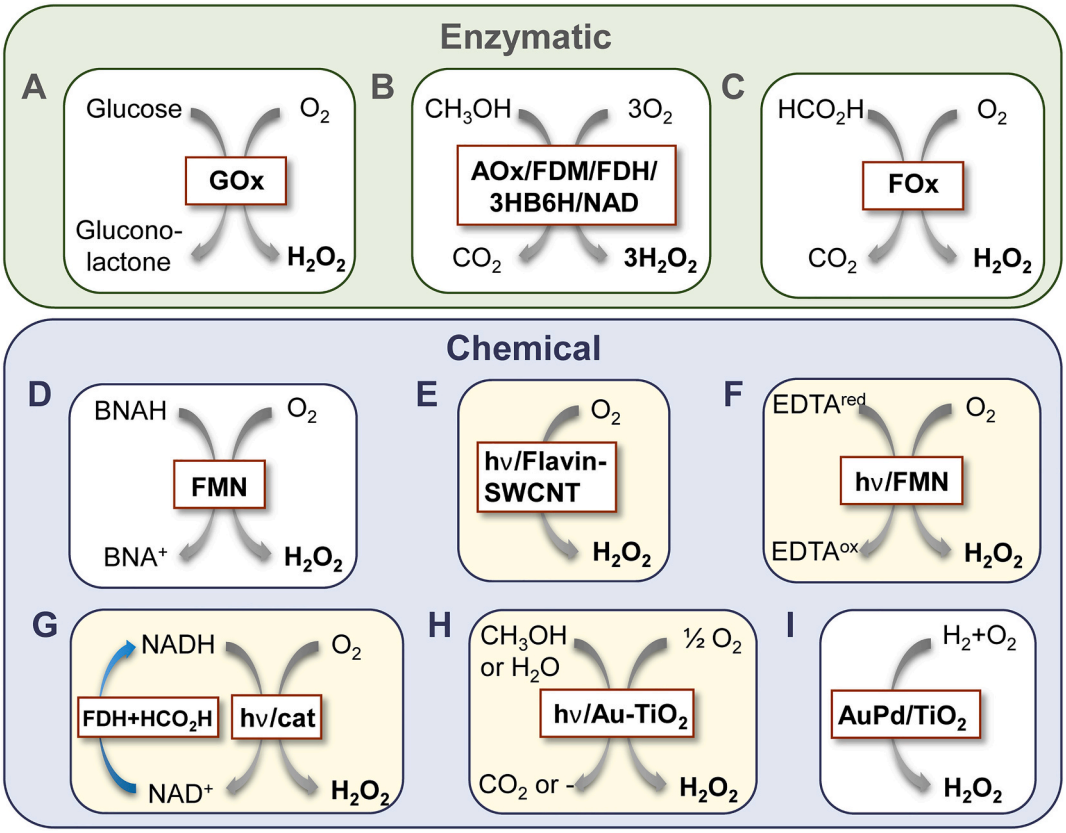

Fig. 8. Schemes of enzymatic and chemical methods for the *in situ* generation of H_2O_2 in peroxygenase reactions. Photoactivation is depicted in yellow background. The enzymatic systems shown are based on glucose oxidation (**A**) by glucose oxidase (GOx) (Kiebist et al., 2017); methanol oxidation (**B**) by a combination of alcohol oxidase (AOx), formaldehyde dismutase (FDM), formate dehydrogenase (FDH) and 3-hydroxybenzoate-6-hydroxylase (3HB6H) (Ni et al., 2016); and formic acid oxidation (**C**) by formate oxidase (FOx) (Tieves et al., 2019). The catalysts used in chemical methods are: **i)** flavins that can be reduced by synthetic nicotinamide cofactors such as BNAH (**D**) (Girhard et al., 2013) or by light when tethered on single-walled carbon nanotubes (SWCNTs) (**E**) (Choi et al., 2017) or in the presence of EDTA (**F**) (Churakova et al., 2011); **(ii)** acridine derivatives as photocalysts combined with FDH systems for NADH regeneration (**G**) (Willot et al., 2019); or **iii)** TiO_2 based catalysts (**H** and **I**) (Freakley et al., 2019; Zhang et al., 2018). (For interpretation of the references to colour in this figure legend, the reader is referred to the web version of this article.)

UPOs in one-pot cascades. Among these methods, the simplicity and catalytic performance of the formate oxidase (FOx) system, which uses just one enzyme and generates volatile CO_2 as by-product is remarkable, achieving high UPO TTNs of 31,800–36,600 in the hydroxylation of ethylbenzene or in the epoxidation of *cis*-β-methylstyrene. Morever, the FOx system circumvents the main disadvantages of traditional methods using glucose oxidase, such as high waste production, low atom efficiency, and increased reaction viscosity by glucose (Tieves et al., 2019).

Many chemical methods are based on the reaction of reduced flavins with O_2 to produce H_2O_2. The reduction of the flavin can be achieved by synthetic nicotinamide cofactors such as 1-benzyl-1,4-dihydronicotinamide (BNAH), like the one reported for hydroxylation of fatty acids with P450-peroxygenases (Girhard et al., 2013) (Fig. 8D), or flavins can be excited by light directly (Fig. 8E) or in the presence of EDTA as electron donor (Fig. 8F). Acridine derivatives have been also used as photocatalysts (Fig. 8G) for H_2O_2 generation, as well as TiO_2-based catalysts (**Fig. 8H** and **I**). High TTNs have been achieved for UPOs in combination with photochemical (38,800-39,900) (Churakova et al., 2011; Willot et al., 2019; Zhang and Hollmann, 2018), photoelectrochemical (123,900) (Choi et al., 2017) and electrochemical (400,000) (Horst et al., 2016) methods for *in situ* H_2O_2 generation, avoiding in the last two cases the formation of by-products. Another remarkable example is the direct generation of H_2O_2 from H_2 and O_2 with supported heterogeneous catalyst (Au-Pd/TiO_2) achieving the highest TTN (61,000) in the hydroxylation of isophorone by UPO (Freakley et al., 2019).

6. Concluding remarks and future trends

The emergence of UPOs represents an important milestone in oxyfunctionalization chemistry because of their unique features, which lead to the selective oxygenation of a variety of compounds in a self-sufficient way only depending on the H_2O_2 oxidizer. Since their discovery in 2004, UPOs have gained more and more importance as promising biocatalysts for industrial applications because, apart from their action on aromatic compounds, their ability to oxygenate aliphatic compounds was demonstrated in 2011. From then on, a wide range of selective oxyfunctionalization (hydroxylation/epoxidation) reactions of aliphatic compounds (fatty acids, fatty alcohols, alkanes, terpenes and steroids) have been reported for the different UPOs that have surfaced throughout this time. Recently, significant advances in understanding the regioselectivity of aliphatic oxygenations have been achieved as a result of structure-function studies based on available UPO crystal structures and computational simulations, which also have directed rational design of the enzymes for improving the selectivity of target reactions, such as the epoxidation of unsaturated fatty acids. In spite of all recent advances in our understanding of UPO catalysis and application, some difficulties are still to be solved, such as the inactivation by hydrogen peroxide that affects enzyme reuse. To deal with this, H_2O_2 is usually continuously pumped or *in situ* generated. With this purpose, several enzymatic and chemical methods have been reported to generate the H_2O_2. In conclusion, these enzymes appear as promising biocatalysts for the environmentally-friendly production of oxyfunctionalized compounds

given their high oxygenating selectivity. Moreover, especially remarkable is the fact that only a few UPOs have been produced and characterized so far, but more than 4000 UPO-encoding genes have been identified in fungal genomes, which entails an important expectation for the future of oxyfunctionalization reactions. Likewise, the availability of more peroxygenase crystal structures in the near future, will provide the opportunity to correlate the different selectivities observed in oxygenation reactions with the architecture of the active site and other structural features. Such information will permit to engineer these self-sufficient monooxygenases (whose activation only depends on a peroxide source) as new and robust industrial biocatalysts for the pharmaceutical and fine-chemical sectors. Finally, whilst companies use their proprietary technologies for large-scale UPO production, a freely-available technology to scale up the production of these enzymes is still lacking.

Acknowledgements

This work has received funding from the Bio Based Industries Joint Undertaking under the European Union's Horizon 2020 research and innovation programme under Grant Agreement No 792063 ("Development and pilot production of sustainable binder systems for wood based panels", https://susbind.eu), and from the Spanish Ministry of Industry, Economy and Competitiveness project BIO2017-86559-R, cofinanced by FEDER funds, and the Consejo Superior de Investigaciones Científicas projects PIE-201620E081 and PIE-202040E185. The authors thank the groups of Victor Guallar (BSC, Barcelona, Spain), Martin Hofrichter (TU Dresden, Zittau, Germany), Katrin Scheibner (JenaBios, Germany), and Frank Hollmann (Delft University, The Netherlands) for their contributions to the IRNAS (Seville, Spain) and CIB (Madrid, Spain) studies on fungal peroxygenases included in the present review. The authors are deeply grateful to Henrik Lund† (Novozymes A/S, Bagsvaerd, Denmark) for his always stimulating support to these studies.

Conflict of interest

None.

References

Acevedo-Rocha, C.G., Gamble, C.G., Lonsdale, R., Li, A., Nett, N., Hoebenreich, S., et al., 2018. P450-catalyzed regio- and diastereoselective steroid hydroxylation: efficient directed evolution enabled by mutability landscaping. ACS Catal. 8, 3395–3410.

Anh, D.H., Ullrich, R., Benndorf, D., Svatos, A., Muck, A., Hofrichter, M., 2007. The coprophilous mushroom *Coprinus radians* secretes a haloperoxidase that catalyzes aromatic peroxygenation. Appl. Environ. Microbiol. 73, 5477–5485.

Anzenbacher, P., Anzenbacherova, E., Lange, R., Skopalik, J., Otyepka, M., 2008. Active sites of cytochromes P450: what are they like? Acta Chim. Slov 55, 63–66.

Aranda, E., Kinne, M., Kluge, M., Ullrich, R., Hofrichter, M., 2009. Conversion of dibenzothiophene by the mushrooms *Agrocybe aegerita* and *Coprinellus radians* and their extracellular peroxygenases. Appl. Microbiol. Biotechnol. 82, 1057–1066.

Aranda, C., del Río, J. C., Gutiérrez, A., Martínez, A. T., 2018a. Process for selective synthesis of 4-hydroxyisophorone and 4-ketoisophorone by fungal peroxygenases. Patent (European) EP1641.1440.

Aranda, C., Municoy, M., Guallar, V., Kiebist, J., Scheibner, K., Ullrich, R., et al., 2018b. Selective synthesis of 4-hydroxyisophorone and 4-ketoisophorone by fungal peroxygenases. Catal. Sci. Technol. 9, 1398–1405.

Aranda, C., Olmedo, A., Kiebist, J., Scheibner, K., del Río, J.C., Martínez, A.T., et al., 2018c. Selective epoxidation of fatty acids and fatty acid methyl esters by fungal peroxygenases. ChemCatChem 10, 3964–3968.

Aranda, C., Ullrich, R., Kiebist, J., Scheibner, K., del Río, J.C., Hofrichter, M., et al., 2018d. Selective synthesis of the resveratrol analogue 4,4′-dihydroxy-*trans*-stilbene and stilbenoids modification by fungal peroxygenases. Catal. Sci. Technol. 8, 2394–2401.

Atrakchi, A.H., 2009. Interpretation and considerations on the safety evaluation of human drug metabolites. Chem. Res. Toxicol. 22, 1217–1220.

Babot, E.D., del Río, J.C., Kalum, L., Martínez, A.T., Gutiérrez, A., 2013. Oxyfunctionalization of aliphatic compounds by a recombinant peroxygenase from *Coprinopsis cinerea*. Biotechnol. Bioeng. 110, 2332.

Babot, E.D., del Río, J.C., Cañellas, M., Sancho, F., Lucas, F., Guallar, V., et al., 2015a. Steroid hydroxylation by basidiomycete peroxygenases: a combined experimental and computational study. Appl. Environ. Microbiol. 81, 4130–4142.

Babot, E.D., del Río, J.C., Kalum, L., Martínez, A.T., Gutiérrez, A., 2015b. Regioselective hydroxylation in the production of 25-hydroxyvitamin D by *Coprinopsis cinerea* peroxygenase. ChemCatChem 7, 283–290.

Babot, E.D., Aranda, C., del Río, J.C., Ullrich, R., Kiebist, J., Scheibner, K., et al., 2020. Selective oxygenation of ionones and damascones by fungal peroxygenases. J. Agric. Food Chem. 68, 5375–5383.

Baillie, T.A., Cayen, M.N., Fouda, H., Gerson, R.J., Green, J.D., Grossman, S.J., et al., 2002. Drug metabolites in safety testing. Toxicology and Applied Pharmacology 182, 188–196.

Balcells, D., Clot, E., Eisenstein, O., 2010. C-H bond activation in transition metal species from a computational perspective. Chem. Rev. 110, 749–823.

Behrendorff, J.B.Y.H., Huang, W., Gillam, E.M.J., 2015. Directed evolution of cytochrome P450 enzymes for biocatalysis: exploiting the catalytic versatility of enzymes with relaxed substrate specificity. Biochemical Journal 467, 1–15.

Belcher, J., McLean, K.J., Matthews, S., Woodward, L.S., Fisher, K., Rigby, S.E.J., et al., 2014. Structure and biochemical properties of the alkene producing cytochrome P450 OleTJE (CYP152L1) from the *Jeotgalicoccus* sp. 8456 bacterium. J. Biol. Chem. 289, 6535–6550.

Bill, R.M., 2014. Playing catch-up with *Escherichia coli*: using yeast to increase success rates in recombinant protein production experiments. Front Microbiol 5, 85.

Blanc, M., Hsieh, W.Y., Robertson, K.A., Kropp, K.A., Forster, T., Shui, G.H., et al., 2013. The transcription factor STAT-1 couples macrophage synthesis of 25-hydroxycholesterol to the interferon antiviral response. Immunity 38, 106–118.

Boddupalli, S.S., Pramanik, B.C., Slaughter, C.A., Estabrook, R.W., Peterson, J.A., 1992. Fatty-acid monooxygenation by P450Bm-3: product identification and proposed mechanisms for the sequential hydroxylation reactions. Arch. Biochem. Biophys. 292, 20–28.

Borugadda, V.B., Goud, V.V., 2014. Epoxidation of castor oil fatty acid methyl esters (COFAME) as a lubricant base stock using heterogeneous ion-exchange resin (IR-120) as a catalyst. Energy Procedia 54, 75–84.

Buck, N. R., Claerhout, W., Leuenberger, B. H., Stoecklin, E., Urban, K., Wolfram, S., 2013. Treating hyperglycemia with 25-hydroxyvitamin D3. Patent (USA)US 20130210782 A1.

Bucko, M., Gemeiner, P., Schenkmayerová, A., Krajcovic, T., Rudroff, F., Mihovilovic, M. D., 2016. Baeyer-Villiger oxidations: biotechnological approach. Applied Microbiology and Biotechnology 100, 6585–6599.

Bureik, M., Bernhardt, R., 2007. Steroid hydroxylation: Microbial steroid biotransformations using cytochrome P450 enzymes, p. 155–176. In: Schmid, R.D., Urlacher, V.B. (Eds.), Modern Biooxidation: Enzymes, Reactions and Applications. Weinheim, Wiley-VCH Verlag GmbH and Co.

Carro, J., Ferreira, P., Rodríguez, L., Prieto, A., Serrano, A., Balcells, B., et al., 2015. 5-Hydroxymethylfurfural conversion by fungal aryl-alcohol oxidase and unspecific peroxygenase. FEBS J. 282, 3218–3229.

Carro, J., Fernández-Fueyo, E., Fernández-Alonso, M.C., Cañada, F.J., Ullrich, R., Hofrichter, M., et al., 2018. Self-sustained enzymatic cascade for the production of 2,5-furandicarboxylic acid from 5-methoxymethylfurfural. Biotechnol. Biofuels 11, 86.

Carro, J., González-Benjumea, A., Fernández-Fueyo, E., Aranda, C., Guallar, V., Gutiérrez, A., et al., 2019. Modulating fatty acid epoxidation *vs* hydroxylation in a fungal peroxygenase. ACS Catal. 9, 6234–6242.

Chakrabarty, S., Wang, Y., Perkins, J.C., Narayan, A.R.H., 2020. Scalable biocatalytic C–H oxyfunctionalization reactions. Chem. Soc. Rev. 49, 8137–8155.

Chen, M.M.Y., Snow, C.D., Vizcarra, C.L., Mayo, S.L., Arnold, F.H., 2012. Comparison of random mutagenesis and semi-rational designed libraries for improved cytochrome P450 BM3-catalyzed hydroxylation of small alkanes. Protein Engineering, Design and Selection 25, 171–178.

Choi, D.S., Ni, Y., Fernández-Fueyo, E., Lee, M., Hollmann, F., Park, C.B., 2017. Photoelectroenzymatic oxyfunctionalization on flavin-hybridized carbon nanotube electrode platform. ACS Catal. 7, 1563–1567.

Churakova, E., Kluge, M., Ullrich, R., Arends, I., Hofrichter, M., Hollmann, F., 2011. Specific photobiocatalytic oxyfunctionalization reactions. Angew. Chem. Int. Ed. 50, 10716–10719.

Ciaramella, A., Minerdi, D., Gilardi, G., 2017. Catalytically self-sufficient cytochromes P450 for green production of fine chemicals. Rendiconti Lincei 28, 169–181.

Colonna, S., Gaggero, N., Casella, L., Carrea, G., Pasta, P., 1992. Chloroperoxidase and hydrogen-peroxide: An efficient system for enzymatic enantioselective sulfoxidations. Tetrahedron-Asymmetry 3, 95–106.

de Gonzalo, G., Mihovilovic, M.D., Fraaije, M.W., 2010. Recent developments in the application of Baeyer-Villiger monooxygenases as biocatalysts. ChemBioChem 11, 2208–2231.

Denisov, I.G., Makris, T.M., Sligar, S.G., Schlichting, I., 2005. Structure and chemistry of cytochrome P450. Chem. Rev. 105, 2253–2277.

Dong, J.J., Fernández-Fueyo, E., Hollmann, F., Paul, C.E., Pesic, M., Schmidt, S., et al., 2018. Biocatalytic oxidation reactions: a chemist's perspective. Angew. Chem. Int. Ed. 57, 9238–9261.

Eggersdorfer, M., Laudert, D., Létinois, U., McClymont, T., Medlock, J., Netscher, T., et al., 2012. One hundred years of vitamins-a success story of the natural sciences. Angew. Chem. Int. Ed. 51, 12960–12990.

Fabara, A.N., Fraaije, M.W., 2020. An overview of microbial indigo-forming enzymes. Appl. Microbiol. Biotechnol. 104, 925–933.

Fegan, K.S., Rae, M.T., Critchley, O.D., Hillier, S.G., 2008. Anti-inflammatory steroid signalling in the human peritoneum. Journal of Endocrinology 196, 369–376.

Fernández-Fueyo, E., Ruiz-Dueñas, F.J., Martínez, M.J., Romero, A., Hammel, K.E., Medrano, F.J., et al., 2014. Ligninolytic peroxidase genes in the oyster mushroom genome: heterologous expression, molecular structure, catalytic and stability properties and lignin-degrading ability. Biotechnol. Biofuels 7, 2.

Fernández-Fueyo, E., Ni, Y., Gomez Baraibar, A., Alcalde, M., van Langen, L.M., Hollmann, F., 2016. Towards preparative peroxygenase-catalyzed oxyfunctionalization reactions in organic media. J. Mol. Catal. B-Enzym. 134 (Part B), 347–352.

Fernández-Fueyo, E., Aranda, C., Gutiérrez, A., Martínez, A. T., 2018. Method of heterologous expression of active fungal unspecific peroxygenase in bacterial host cells for fatty-acid epoxidation and other oxygenation reactions. Patent (European) EP18382514.0.

Freakley, S.J., Kochius, S., van Marwijk, J., Fenner, C., Lewis, R.J., Baldenius, K., et al., 2019. A chemo-enzymatic oxidation cascade to activate C-H bonds with in situ generated H_2O_2. Nat. Commun. 10, 4178.

Fujishiro, T., Shoji, O., Nagano, S., Sugimoto, H., Shiro, Y., Watanabe, Y., 2011. Crystal structure of H_2O_2-dependent cytochrome $P450_{SP\alpha}$ with its bound fatty acid substrate: insight into the regioselective hydroxylation of fatty acids at the α-position. J. Biol. Chem. 286, 29941–29950.

Fujishiro, T., Shoji, O., Kawakami, N., Watanabe, T., Sugimoto, H., Shiro, Y., Watanabe, Y., 2012. Chiral-substrate-assisted stereoselective epoxidation catalyzed by H_2O_2-dependent cytochrome $P450_{SP\alpha}$. Chem.Asian J. 10, 2286–2293 (7-10-2012).

Fürst, M.J.L.J., Kerschbaumer, B., Rinnofner, C., Migglautsch, A.K., Winkler, M., Fraaije, M.W., 2019. Exploring the biocatalytic potential of a self-sufficient cytochrome P450 from *Thermothelomyces thermophila*. Adv. Synth. Catal. 361, 2487–2496.

Geigert, J., Lee, T.D., Dalietos, D.J., Hirano, D.S., Neidleman, S.L., 1986. Epoxidation of alkenes by chloroperoxidase catalysis. Biochemical and Biophysical Research Communications 136, 778–782.

Girhard, M., Schuster, S., Dietrich, M., Dürre, P., Urlacher, V.B., 2007. Cytochrome P450 monooxygenase from *Clostridium acetobutylicum*: a new α-fatty acid hydroxylase. Biochemical and Biophysical Research Communications 362, 114–119.

Girhard, M., Kunigk, E., Tihovsky, S., Shumyantseva, V.V., Urlacher, V.B., 2013. Light-driven biocatalysis with cytochrome P450 peroxygenases. Biotechnol. Appl. Bioc. 60, 111–118.

Girhard, M., Bakkes, P.J., Mahmoud, O., Urlacher, V., 2015. P450 biotechnology, p. 451–520. In: Ortiz de Montellano, P.R. (Ed.), Cytochrome P450 Structure, Mechanism, and Biochemistry. Springer.

Girvan, H.M., Seward, H.E., Toogood, H.S., Cheesman, M.R., Leys, D., Munro, A.W., 2007. Structural and spectroscopic characterization of P450 BM3 mutants with unprecedented P450 heme iron ligand sets: new heme ligation states influence conformational equilibria in P450 BM3. J. Biol. Chem. 282, 564–572.

Gómez de Santos, P., Molina-Espeja, P., Plou, F. J., Alcalde, M., 2018. Regioselective synthesis of 5′-hydroxypropranolol by aromatic peroxygenase designed by directed evolution. Patent (Spain) P300212672.

González-Benjumea, A., Carro, J., Renau, C., Linde, D., Fernández-Fueyo, E., Gutiérrez, A., et al., 2020. Fatty acid epoxidation by the new *Collariella virescens* peroxygenase and heme-channel variants. Catal. Sci. Technol. 10, 717–725.

González-Benjumea, A., Marques, G., Herold-Majumdar, O.M., Kiebist, J., Scheibner, K., del Río, J.C., et al., 2021. High epoxidation yields of vegetable oil hydrolyzates and methyl esters by selected fungal peroxygenases. Front. Bioeng. Biotechnol. 8, 605854.

González-Pérez, D., Molina-Espeja, P., García-Ruiz, E., Alcalde, M., 2014. Mutagenic organized recombination process by homologous in vivo grouping (MORPHING) for directed enzyme evolution. PLoS ONE 9, 3–e90919.

Gröbe, G., Ullrich, M., Pecyna, M., Kapturska, D., Friedrich, S., Hofrichter, M., et al., 2011. High-yield production of aromatic peroxygenase by the agaric fungus *Marasmius rotula*. AMB Express 1, 31–42.

Guengerich, F.P., Waterman, M.R., Egli, M., 2016. Recent structural insights into cytochrome P450 function. Trends in Pharmacological Sciences 37, 625–640.

Gutiérrez, A., Babot, E.D., Ullrich, R., Hofrichter, M., Martínez, A.T., del Río, J.C., 2011. Regioselective oxygenation of fatty acids, fatty alcohols and other aliphatic compounds by a basidiomycete heme-thiolate peroxidase. Arch. Biochem. Biophys. 514, 33–43.

Hamberg, M., Fahlstadius, P., 1992. On the specificity of a fatty acid epoxygenase in broad bean (*Vicia faba* L.). Plant Physiol 99, 987–995.

Hammerer, L., Winkler, C.K., Kroutil, W., 2018. Regioselective biocatalytic hydroxylation of fatty acids by cytochrome P450s. Catalysis Letters 148, 787–812.

Hofrichter, M., Kellner, H., Pecyna, M.J., Ullrich, R., 2015. Fungal unspecific peroxygenases: Heme-thiolate proteins that combine peroxidase and cytochrome P450 properties. Adv. Exp. Med. Biol. 851, 341–368.

Hofrichter, M., Kellner, H., Herzog, R., Karich, A., Liers, C., Scheibner, K., et al., 2020. Fungal peroxygenases: A phylogenetically old superfamily of heme enzymes with promiscuity for oxygen transfer reactions. In: Nevalainen, H. (Ed.), Grand Challenges in Fungal Biotechnology. Springer, Cham, Switzerland, pp. 369–403.

Holtmann, D., Hollmann, F., 2016. The oxygen dilemma: a severe challenge for the application of monooxygenases? ChemBioChem 17, 1391–1398.

Horst, A.E.W., Bormann, S., Meyer, J., Steinhagen, M., Ludwig, R., Drews, A., et al., 2016. Electro-enzymatic hydroxylation of ethylbenzene by the evolved unspecific peroxygenase of *Agrocybe aegerita*. Journal of Molecular Catalysis B: Enzymatic 133, S137–S142.

Huang, W.C., Cullis, P.M., Raven, E.L., Roberts, G.C.K., 2011. Control of the stereo-selectivity of styrene epoxidation by cytochrome P450 BM3 using structure-based mutagenesis. Metallomics 3, 410–416.

Huijbers, M.M.E., Montersino, S., Westphal, A.H., Tischler, D., van Berkel, W.J.H., 2014. Flavin dependent monooxygenases. Arch. Biochem. Biophys. 544, 2–17.

Isler, O., Lindlar, H., Montavon, M., Rüegg, R., Saucy, G., Zeller, P., 1956. Synthesen in der carotinoid-reihe mitteilung. Totalsynthese von zeaxanthin und physalien. HCA 39, 2041–2053.

Jean, G., Charra, B., Chazot, C., 2008. Vitamin D deficiency and associated factors in hemodialysis patients. Journal of Renal Nutrition 18, 395–399.

Jia, P., Zhang, M., Hu, L., Zhou, Y., 2016. Green plasticizers derived from soybean oil for poly(vinyl chloride) as a renewable resource material. Korean Journal of Chemical Engineering 33, 1080–1087.

Johnson, E.F., Stout, C.D., 2013. Structural diversity of eukaryotic membrane cytochrome P450s. Journal of Biological Chemistry 288, 17082–17090.

Jones, G., 2013. Extrarenal vitamin D activation and interactions between vitamin D-2, vitamin D-3, and vitamin D analogs. Annu. Rev. Nutr. 33, 23–44.

Kaluzna, I., Schmitges, T., Straatman, H., van Tegelen, D., Müller, M., Schürmann, M., et al., 2016. Enabling selective and sustainable P450 oxygenation technology. Production of 4-hydroxy-α-isophorone on kilogram scale. Org. Process Res. Dev. 20, 814–819.

Kandula, S., Stolp, L., Grass, M., Woldt, B., Kodali, D., 2014. Synthesis and functional evaluation of soy fatty acid methyl ester ketals as bioplasticizers. Journal of the American Oil Chemists' Society 91, 1967–1974.

Karich, A., Kluge, M., Ullrich, R., Hofrichter, M., 2013. Benzene oxygenation and oxidation by the peroxygenase of *Agrocybe aegerita*. AMB Express 3, 5.

Keenaan, C., Zhang, H., Shea, E.V., Hollenberg, P.F., 2011. Uncovering the role of hydrophobic residues in cytochrome P450-cytochrome P450 reductase interactions. Biochemistry 50, 3957–3967.

Kiebist, J., Schmidtke, K.U., Zimmermann, J., Kellner, H., Jehmlich, N., Ullrich, R., et al., 2017. A peroxygenase from *Chaetomium globosum* catalyzes the selective oxygenation of testosterone. ChemBioChem 18, 563–569.

Kille, S., Zilly, F.E., Acevedo, J.P., Reetz, M.T., 2011. Regio- and stereoselectivity of P450-catalysed hydroxylation of steroids controlled by laboratory evolution. Nature Chemistry 3, 738–743.

Kinne, M., Ullrich, R., Hammel, K.E., Scheibner, K., Hofrichter, M., 2008. Regioselective preparation of (*R*)-2-(4-hydroxyphenoxy)propionic acid with a fungal peroxygenase. Tetrahedron Lett. 49, 5950–5953.

Kinne, M., Poraj-Kobielska, M., Ralph, S.A., Ullrich, R., Hofrichter, M., Hammel, K.E., 2009. Oxidative cleavage of diverse ethers by an extracellular fungal peroxygenase. J. Biol. Chem. 284, 29343–29349.

Kinne, M., Zeisig, C., Ullrich, R., Kayser, G., Hammel, K.E., Hofrichter, M., 2010. Stepwise oxygenations of toluene and 4-nitrotoluene by a fungal peroxygenase. Biochem. Biophys. Res. Commun. 397, 18–21.

Kluge, M., Ullrich, R., Dolge, C., Scheibner, K., Hofrichter, M., 2009. Hydroxylation of naphthalene by aromatic peroxygenase from *Agrocybe aegerita* proceeds via oxygen transfer from H_2O_2 and intermediary epoxidation. Appl. Microbiol. Biotechnol. 81, 1071–1076.

Kluge, M., Ullrich, R., Scheibner, K., Hofrichter, M., 2012. Stereoselective benzylic hydroxylation of alkylbenzenes and epoxidation of styrene derivatives catalyzed by the peroxygenase of *Agrocybe aegerita*. Green Chem. 14, 440–446.

Kubo, T., Peters, M.W., Meinhold, P., Arnold, F.H., 2006. Enantioselective epoxidation of terminal alkenes to (*R*)- and (*S*)-epoxides by engineered cytochromes P450 BM-3. Chem. Eur. J. 12, 1216–1220.

Kubota, M., Nodate, M., Yasumoto-Hirose, M., Uchiyama, T., Kagami, O., Shizuri, Y., et al., 2005. Isolation and functional analysis of cytochrome P450 CYP153A genes from various environments. Null 69, 2421–2430.

Lambertz, C., Garvey, M., Klinger, J., Heesel, D., Klose, H., Fischer, R., et al., 2014. Challenges and advances in the heterologous expression of cellulolytic enzymes: a review. Biotechnol Biofuels 7, 135.

Lecina, D., Gilabert, J.F., Guallar, V., 2017. Adaptive simulations, towards interactive protein-ligand modeling. Sci. Rep. 7, 8466.

Lentz, O., Feenstra, A., Habicher, T., Hauer, B., Schmid, R.D., Urlacher, V.B., 2006. Altering the regioselectivity of cytochrome P450 CYP102A3 of *Bacillus subtilis* by using a new versatile assay system. ChemBioChem 7, 345–350.

Li, Q.S., Ogawa, J., Shimizu, S., 2001. Critical role of the residue size at position 87 in H_2O_2-dependent substrate hydroxylation activity and H_2O_2 inactivation of cytochrome P450BM-3. Biochemical and biophysical research communications 280, 1258–1261.

Lin, H., Tang, D.F., Ahmed, A.A.Q., Liu, Y., Wu, Z.L., 2012. Mutations at the putative active cavity of styrene monooxygenase: enhanced activity and reversed enantioselectivity. Journal of Biotechnology 161, 235–241.

Linde, D., Coscolín, C., Liers, C., Hofrichter, M., Martínez, A.T., Ruiz-Dueñas, F.J., 2014. Heterologous expression and physicochemical characterization of a fungal dye-decolorizing peroxidase from *Auricularia auricula-judae*. Protein Express. Purif. 103, 28–37.

Linde, D., Olmedo, A., González-Benjumea, A., Renau, C., Estévez, M., Carro, J., et al., 2020. Two new unspecific peroxygenases from heterologous expression of fungal genes in *Escherichia coli*. Appl. Environ. Microbiol. 86 https://doi.org/10.1128/AEM.02899-19.

Liu, S.Y., Aliyari, R., Chikere, K., Li, G.M., Marsden, M.D., Smith, J.K., et al., 2013. Interferon-inducible cholesterol-25-hydroxylase broadly inhibits viral entry by production of 25-hydroxycholesterol. Immunity 38, 92–105.

Liu, X., Wang, Z.B., Wang, Y.N., Kong, J.Q., 2016a. Probing steroidal substrate specificity of cytochrome P450 BM3 variants. Molecules 21, 760. https://doi.org/10.3390/molecules21060760.

Liu, Y., Liu, Y.C., Wu, Z.L., 2016b. Asymmetric bio-epoxidation catalyzed with the styrene monooxygenase from *Pseudomonas* sp. LQ26. Bioresources and Bioprocessing 3, 10.

Lucas, F., Babot, E.D., del Río, J.C., Kalum, L., Ullrich, R., Hofrichter, M., et al., 2016. Molecular determinants for selective C25-hydroxylation of vitamins D2 and D3 by fungal peroxygenases. Catal. Sci. Technol. 6, 288–295.

Manoj, K.M., Hager, L.P., 2001. Utilization of peroxide and its relevance in oxygen insertion reactions catalyzed by chloroperoxidase. Biochimica et Biophysica Acta (BBA) - Protein Structure and Molecular Enzymology 1547, 408–417.
Martín-Díaz, J., Paret, C., García-Ruiz, E., Molina-Espeja, P., Alcalde, M., 2018. Shuffling the neutral drift of unspecific peroxygenase in *Saccharomyces cerevisiae*. Appl. Environ. Microbiol. 84, e00808–e00818.
Matsunaga, I., Kusunose, E., Yano, I., Ichihara, K., 1994. Separation and partial characterization of soluble fatty acid a-hydroxylase from *Sphingomonas paucimobilis*. Biochem. Biophys. Res. Commun. 201, 1554–1560.
Matsunaga, I., Ueda, A., Fujiwara, N., Sumimoto, T., Ichihara, K., 1999. Characterization of the *ybdT* gene product of *Bacillus subtilis*: novel fatty acid β-hydroxylating cytochrome P450. Lipids 34 (8), 841–846.
McKenna, R., Pugh, S., Thompson, B., Nielsen, D.R., 2013. Microbial production of the aromatic building-blocks (S)-styrene oxide and (R)-1,2-phenylethanediol from renewable resources. Biotechnology Journal 8, 1465–1475.
Meinhold, P., Peters, M.W., Hartwick, A., Hernandez, A.R., Arnold, F., 2006. Engineering cytochrome P450 BM3 for terminal alkane hydroxylation. Adv. Synth. Catal. 348, 763–772.
Metzger, J.O., Bornscheuer, U., 2006. Lipids as renewable resources: current state of chemical and biotechnological conversion and diversification. Applied Microbiology and Biotechnology 71, 13–22.
Miki, Y., Morales, M., Ruiz-Dueñas, F.J., Martínez, M.J., Wariishi, H., Martínez, A.T., 2009. *Escherichia coli* expression and in vitro activation of a unique ligninolytic peroxidase that has a catalytic tyrosine residue. Protein Express. Purif. 68, 208–214.
Miller, V.P., Tschirretguth, R.A., Ortiz de Montellano, P.R., 1995. Chloroperoxidase-catalyzed benzylic hydroxylation. Archives of Biochemistry and Biophysics 319, 333–340.
Miura, Y., Fulco, A.J., 1975. ω-1, ω-2 and ω-3 hydroxylation of long-chain fatty-acids, amides and alcohols by a soluble enzyme-system from *Bacillus megaterium*. Biochim. Biophys. Acta-Lipids Lipid Metab. 388, 305–317.
Molina-Espeja, P., Garcia-Ruiz, E., Gonzalez-Perez, D., Ullrich, R., Hofrichter, M., Alcalde, M., 2014. Directed evolution of unspecific peroxygenase from *Agrocybe aegerita*. Appl. Environ. Microbiol. 80, 3496–3507.
Molina-Espeja, P., Ma, S., Maté, D.M., Ludwig, R., Alcalde, M., 2015a. Tandem-yeast expression system for engineering and producing unspecific peroxygenase. Enzyme Microb. Technol. 73–74, 29–33.
Molina-Espeja, P., Plou, F., Alcalde, M., Gómez de Santos, P., 2015b. Mutants of unspecific peroxygenase with high monooxygenase activity and uses thereof. Patent (International) WO 2017/081355 A1.
Mooney, A., Ward, P.G., O'Connor, K.E., 2006. Microbial degradation of styrene: biochemistry, molecular genetics, and perspectives for biotechnological applications. Applied Microbiology and Biotechnology 72, 1–10.
Municoy, M., González-Benjumea, A., Carro, J., Aranda, C., Linde, D., Renau-Mínguez, C., et al., 2020. Fatty-acid oxygenation by fungal peroxygenases: from computational simulations to preparative regio- and stereo-selective epoxidation. ACS Catal. 10, 13584–13595.
Munro, A.W., McLean, K.J., Grant, J.L., Makris, T.M., 2018. Structure and function of the cytochrome P450 peroxygenase enzymes. Biochem. Soc. Trans. 46, 183–196.
Murphy, R.C., Johnson, K.M., 2008. Cholesterol, reactive oxygen species, and the formation of biologically active mediators. Journal of Biological Chemistry 283, 15521–15525.
Mutlu, H., Meier, M.A.R., 2010. Castor oil as a renewable resource for the chemical industry. Eur. J. Lipid Sci. Technol. 112, 10–30.
Neufeld, K., Marienhagen, J., Schwaneberg, U., Pietruszka, J., 2013. Benzylic hydroxylation of aromatic compounds by P450 BM3. Green Chem. 15, 2408–2421.
Ni, Y., Fernández-Fueyo, E., Baraibar, A.G., Ullrich, R., Hofrichter, M., Yanase, H., et al., 2016. Peroxygenase-catalyzed oxyfunctionalization reactions promoted by the complete oxidation of methanol. Angew. Chem. Int. Ed. 55, 798–801.
Olmedo, A., Aranda, C., del Río, J.C., Kiebist, J., Scheibner, K., Martínez, A.T., et al., 2016. From alkanes to carboxylic acids: terminal oxygenation by a fungal peroxygenase. Angew. Chem. Int. Ed. 55, 12248–12251.
Olmedo, A., del Río, J.C., Kiebist, J., Scheibner, K., Martínez, A.T., Gutiérrez, A., 2017. Fatty acid chain shortening by a fungal peroxygenase. Chem. Eur. J. 23, 16985–16989.
Pecyna, M.J., Ullrich, R., Bittner, B., Clemens, A., Scheibner, K., Schubert, R., et al., 2009. Molecular characterization of aromatic peroxygenase from *Agrocybe aegerita*. Appl. Microbiol. Biotechnol. 84, 885–897.
Pennec, A., Jacobs, C.L., Opperman, D.J., Smit, M.S., 2015. Revisiting cytochrome P450-mediated oxyfunctionalization of linear and cyclic alkanes. Adv. Synth. Catal. 357, 118–130.
Pérez-Boada, M., Doyle, W.A., Ruiz-Dueñas, F.J., Martínez, M.J., Martínez, A.T., Smith, A.T., 2002. Expression of *Pleurotus eryngii* versatile peroxidase in *Escherichia coli* and optimisation of *in vitro* folding. Enzyme Microb. Technol. 30, 518–524.
Peter, S., Kinne, M., Wang, X., Ulrich, R., Kayser, G., Groves, J.T., et al., 2011. Selective hydroxylation of alkanes by an extracellular fungal peroxygenase. FEBS J. 278, 3667–3675.
Peter, S., Karich, A., Ullrich, R., Gröbe, G., Scheibner, K., Hofrichter, M., 2014. Enzymatic one-pot conversion of cyclohexane into cyclohexanone: Comparison of four fungal peroxygenases. J. Mol. Catal. B-Enzym. 103, 47–51 (online).
Peter, S., Kinne, M., Ullrich, R., Kayser, G., Hofrichter, M., 2013. Epoxidation of linear, branched and cyclic alkenes catalyzed by unspecific peroxygenase. Enzyme Microb. Technol. 52, 370–376.
Piontek, K., Ullrich, R., Liers, C., Diederichs, K., Plattner, D.A., Hofrichter, M., 2010. Crystallization of a 45 kDa peroxygenase/peroxidase from the mushroom *Agrocybe aegerita* and structure determination by SAD utilizing only the haem iron. Acta Crystallogr. F 66, 693–698.
Piontek, K., Strittmatter, E., Ullrich, R., Gröbe, G., Pecyna, M.J., Kluge, M., et al., 2013. Structural basis of substrate conversion in a new aromatic peroxygenase: cytochrome P450 functionality with benefits. J. Biol. Chem. 288, 34767–34776.
Poraj-Kobielska, M., Kinne, M., Ullrich, R., Scheibner, K., Kayser, G., Hammel, K.E., et al., 2011. Preparation of human drug metabolites using fungal peroxygenases. Biochem. Pharmacol. 82, 789–796.
Poulos, T.L., 2005. Structural biology of heme monooxygenases. Biochemical and Biophysical Research Communications 338, 337–345.
Püllmann, P., Knorrscheidt, A., Münch, J., Palme, P.R., Hoehenwarter, W., Marillonnet, S., et al., 2020. A modular two yeast species secretion system for the production and preparative application of fungal peroxygenases. bioRxiv. https://doi.org/10.1101/2020.07.22.216432.
Ramírez-Escudero, M., Molina-Espeja, P., Gómez de Santos, P., Hofrichter, M., Sanz-Aparicio, J., Alcalde, M., 2018. Structural insights into the substrate promiscuity of a laboratory evolved peroxygenase. ACS Chem. Biol. 13, 3259–3268.
Rauch, M.C.R., Tieves, F., Paul, C.E., Arends, I.W.C.E., Alcalde, M., Hollmann, F., 2019. Peroxygenase-catalysed epoxidation of styrene derivatives in neat reaction media. ChemCatChem 11, 4519–4523.
Rea, V., Kolkman, A.J., Vottero, E., Stronks, E.J., Ampt, K.A.M., Honing, M., et al., 2012. Active site substitution A82W improves the regioselectivity of steroid hydroxylation by cytochrome P450 BM3 mutants as rationalized by spin relaxation nuclear magnetic resonance studies. Biochemistry 51, 750–760.
Rinnofner, C., Kerschbaumer, B., Weber, H., Glieder, A., Winkler, M., 2019. Cytochrome P450 mediated hydroxylation of ibuprofen using *Pichia pastoris* as biocatalyst. Biocatalysis and Agricultural Biotechnology 17, 525–528.
Roberts, G.A., Çelik, A., Hunter, D.J.B., Ost, T.W.B., White, J.H., Chapman, S.K., et al., 2003. A self-sufficient cytochrome P450 with a primary structural organization that includes a flavin domain and a [2Fe-2S] redox center. Journal of Biological Chemistry 278, 48914–48920.
Robin, A., Köhler, V., Jones, A., Ali, A., Kelly, P.P., O'Really, E., Turner, N.J., Flitsch, S. L., 2011. Chimeric self-sufficient P450cam-RhFRed biocatalysts with broad substrate scope. Belstein J.Org.Chem. 7, 1494–1498.
Roduner, E., Kaim, W., Sarkar, B., Urlacher, V.B., Pleiss, J., Gläser, R., et al., 2013. Selective catalytic oxidation of C-H bonds with molecular oxygen. ChemCatChem 5, 82–112.
Sadeghi, S.J., Gilardi, G., 2013. Chimeric P450 enzymes: activity of artificial redox fusions driven by different reductases for biotechnological applications. Biotechnology and Applied Biochemistry 60, 102–110.
Seifert, A., Antonovici, M., Hauer, B., Pleiss, J., 2011. An efficient route to selective bio-oxidation catalysts: an iterative approach comprising modeling, diversification, and screening, based on CYP102A1. ChemBioChem 12, 1346–1351.
Serra, S., De Simeis, D., 2019. Fungi-mediated biotransformation of the isomeric forms of the apocarotenoids ionone, damascone and theaspirane. Molecules 24, 19.
Shaik, S., Kumar, D., de Visser, S.P., Altun, A., Thiel, W., 2005. Theoretical perspective on the structure and mechanism of cytochrome P450 enzymes. Chem. Rev. 105, 2279–2328.
Sheldon, R.A., Woodley, J.M., 2018. Role of biocatalysis in sustainable chemistry. Chem. Rev. 118, 801–838.
Šrejber, M., Navrátilová, V., Paloncýová, M., Bazgier, V., Berka, K., Anzenbacher, P., et al., 2018. Membrane-attached mammalian cytochromes P450: an overview of the membrane's effects on structure, drug binding, and interactions with redox partners. Journal of Inorganic Biochemistry 183, 117–136.
Syed, K., Mashele, S.S., 2014. Comparative analysis of P450 signature motifs EXXR and CXG in the large and diverse kingdom of fungi: identification of evolutionarily conserved amino acid patterns characteristic of P450 family. PLoS One 9, e95616.
Tavanti, M., Porter, J.L., Sabatini, S., Turner, N.J., Flitsch, S.L., 2018. Panel of new thermostable CYP116B self-sufficient cytochrome P450 monooxygenases that catalyze C-H activation with a diverse substrate scope. ChemCatChem 10, 1042–1051.
Tieves, F., Willot, S.J.P., van Schie, M.M.C.H., Rauch, M.C.R., Younes, S.H.H., Zhang, W. Y., et al., 2019. Formate oxidase (FOx) from aspergillus oryzae: one catalyst enables diverse H2O2-dependent biocatalytic oxidation reactions. Angew. Chem. Int. Ed. 58, 7873–7877.
Tiran, C., Lecomte, J., Dubreucq, E., Villeneuve, P., 2008. Chemo-enzymatic epoxidation of fatty compounds- focus on processes involving a lipase-catalyzed perhydrolysis step. OCL 15, 179–183.
Toda, H., Imae, R., Itoh, N., 2012a. Efficient biocatalysis for the production of enantiopure *(S)*-epoxides using a styrene monooxygenase (SMO) and *Leifsonia* alcohol dehydrogenase (LSADH) system. Tetrahedron: Asymmetry 23, 1542–1549.
Toda, H., Imae, R., Komio, T., Itoh, N., 2012b. Expression and characterization of styrene monooxygenases of *Rhodococcus* sp. ST-5 and ST-10 for synthesizing enantiopure *(S)*-epoxides. Applied Microbiology and Biotechnology 96, 407–418.
Toda, H., Ohuchi, T., Imae, R., Itoh, N., 2015. Microbial production of aliphatic (*S*)-epoxyalkanes by using *Rhodococcus* sp. strain ST-10 styrene monooxygenase expressed in organic-solvent-tolerant *Kocuria rhizophila* DC2201. Appl. Environ. Microbiol. 81, 1919.
Tuynman, A., Spelberg, J.L., Kooter, I.M., Schoemaker, H.E., Wever, R., 2000. Enantioselective epoxidation and carbon-carbon bond cleavage catalyzed by *Coprinus cinereus* peroxidase and myeloperoxidase. Journal of Biological Chemistry 275, 3025–3030.
Ullrich, R., Hofrichter, M., 2005. The haloperoxidase of the agaric fungus *Agrocybe aegerita* hydroxylates toluene and naphthalene. FEBS Lett. 579, 6247–6250.
Ullrich, R., Nuske, J., Scheibner, K., Spantzel, J., Hofrichter, M., 2004. Novel haloperoxidase from the agaric basidiomycete *Agrocybe aegerita* oxidizes aryl alcohols and aldehydes. Appl. Environ. Microbiol. 70, 4575–4581.

Ullrich, R., Dolge, C., Kluge, M., Hofrichter, M., 2008. Pyridine as novel substrate for regioselective oxygenation with aromatic peroxygenase from *Agrocybe aegerita*. FEBS Lett. 582, 4100–4106.
Ullrich, R., Poraj-Kobielska, M., Scholze, S., Halbout, C., Sandvoss, M., Pecyna, M.J., et al., 2018. Side chain removal from corticosteroids by unspecific peroxygenase. Journal of Inorganic Biochemistry 183, 84–93.
Urban, P., Lautier, T., Pompon, D., Truan, G., 2018. Ligand access channels in cytochrome P450 enzymes: a review. Int. J. Molec. Sci. 19.
Urlacher, V.B., Makhsumkhanov, A., Schmid, R.D., 2006. Biotransformation of β-ionone by engineered cytochrome P450 BM-3. Appl. Microbiol. Biotechnol. 70, 53–59.
Vandamme, E.J., Soetaert, W., 2002. Bioflavours and fragrances via fermentation and biocatalysis. J. Chem. Technol. Biotechnol. 77, 1323–1332.
Venkataraman, H., de Beer, S.B.A., van Bergen, L.A.H., van Essen, N., Geerke, D.P., Vermeulen, N.P.E., et al., 2012. A single active site mutation inverts stereoselectivity of 16-hydroxylation of testosterone catalyzed by engineered cytochrome P450 BM3. ChemBioChem 13, 520–523.
Vottero, E., Rea, V., Lastdrager, J., Honing, M., Vermeulen, N.P.E., Commandeur, J.N.M., 2011. Role of residue 87 in substrate selectivity and regioselectivity of drug-metabolizing cytochrome P450 CYP102A1 M11. JBIC Journal of Biological Inorganic Chemistry 16, 899–912.
Wang, Y., Lan, D., Durrani, R., Hollmann, F., 2017. Peroxygenases en route to becoming dream catalysts. What are the opportunities and challenges? Curr. Opin. Chem. Biol. 37, 1–9.
Weber, E., Seifert, A., Antonovici, M., Geinitz, C., Pleiss, J., Urlacher, V.B., 2011. Screening of a minimal enriched P450 BM3 mutant library for hydroxylation of cyclic and acyclic alkanes. Chem. Commun. 47, 944–946.
Wei, Y., Ang, E.L., Zhao, H., 2018. Recent developments in the application of P450 based biocatalysts. Current Opinion in Chemical Biology 43, 1–7.
Whitehouse, C.J.C., Bell, S.G., Wong, L.L., 2012. P450(BM3) (CYP102A1): connecting the dots. Chem. Soc. Rev. 41, 1218–1260.
Willot, S.J.P., Fernández-Fueyo, E., Tieves, F., Pesic, M., Alcalde, M., Arends, I.W.C.E., et al., 2019. Expanding the spectrum of light-driven peroxygenase reactions. ACS Catal. 9, 890–894.
Wiltschi, B., Cernava, T., Dennig, A., Galindo Casas, M., Geier, M., Gruber, S., et al., 2020. Enzymes revolutionize the bioproduction of value-added compounds: from enzyme discovery to special applications. Biotechnology Advances 40, 107520.
Wohlgemuth, R., 2017. Biocatalytic process design and reaction engineering. Chem. Biochem. Eng. Q 31, 131–138.
Woodley, J.M., 2019. Reaction engineering for the industrial implementation of biocatalysis. Topics in Catalysis 62, 1207.
Xia, Y., Larock, R.C., 2010. Vegetable oil-based polymeric materials: synthesis, properties, and applications. Green Chem. 12, 1893–1909.
Xu, L.H., Du, Y.L., 2018. Rational and semi-rational engineering of cytochrome P450s for biotechnological applications. Synthetic and Systems Biotechnology 3, 283–290.
Xue, X.S., Ji, P., Zhou, B., Cheng, J.P., 2017. The essential role of bond energetics in C-H activation/functionalization. Chem. Rev. 117, 8622–8648.
Yin, Y.C., Yu, H.L., Luan, Z.J., Li, R.J., Ouyang, P.F., Liu, J., et al., 2014. Unusually broad substrate profile of self-sufficient cytochrome P450 monooxygenase CYP116B4 from *Labrenzia aggregata*. ChemBioChem 15, 2443–2449.
Zhang, W.Y., Hollmann, F., 2018. Nonconventional regeneration of redox enzymes - a practical approach for organic synthesis? Chem. Commun. 54, 7281–7289.
Zhang, C., Ding, R., Kessler, M.R., 2014a. Reduction of epoxidized vegetable oils: a novel method to prepare bio-based polyols for polyurethanes. Macromol. Rapid Commun. 35, 1068–1074.
Zhang, C., Li, Y., Chen, R., Kessler, M.R., 2014b. Polyurethanes from solvent-free vegetable oil-based polyols. ACS Sustain. Chem. Eng. 2, 2465–2476.
Zhang, W., Fernández-Fueyo, E., Ni, Y., van Schie, M., Gacs, J., Renirie, R., et al., 2018. Selective aerobic oxidation reactions using a combination of photocatalytic water oxidation and enzymatic oxyfunctionalizations. Nature Catalysis 1, 55–62.